NUMERICAL HARTREE-FOCK-SLATER CALCULATIONS ON DIATOMIC MOLECULES

By

© AXEL DIETER BECKE, B.Sc., M.Sc.

A Thesis

Submitted to the School of Graduate Studies

in Partial Fulfilment of the Requirements

for the Degree

Doctor of Philosophy

McMaster University

July 1981

DOCTOR OF PHILOSOPHY (1981) McMASTER UNIVERSITY
(Physics) Hamilton, Ontario

TITLE: Numerical Hartree-Fock-Slater Calculations on Diatomic Molecules

AUTHOR: Axel Dieter Becke, B.Sc. (Queen's University)
M.Sc. (McMaster University)

SUPERVISOR: Dr. D.W.L. Sprung

NUMBER OF PAGES: vi , 104

ABSTRACT

A completely numerical method has been developed for the calculation of Hartree-Fock-Slater wave functions in diatomic systems. The method is numerical in the sense that no LCAO basis sets are employed. All molecular functions are represented by cubic spline interpolants on a two-dimensional discrete mesh in prolate spheroidal coordinates. The method is mathematically simple, and numerical accuracy is very easily controlled by adjusting the number of mesh points. Furthermore, it is easily applied to other local exchange-correlation theories beyond the Hartree-Fock-Slater approximation.

Calculations on the molecules B_2, C_2, N_2, CO, O_2 and F_2 have been carried out in order to compare dissociation energies, bond lengths, vibrational frequencies and quadrupole (or dipole) moments with recently reported LCAO results, and with experiment. These calculations indicate that the present numerical method works very nicely for the molecules considered, and also that the Hartree-Fock-Slater theory describes molecular systems remarkably well.

ACKNOWLEDGEMENTS

I would like to thank my supervisor, Dr. D.W.L. Sprung, for his assistance and support of this research, and also the members of my supervisory committee, Drs. R.K. Bhaduri, R.F.W. Bader, and D.P. Santry. Thanks also to Dr. Tom Ziegler for particularly helpful discussions.

I am very grateful to the McMaster theoretical physics group for providing a most pleasant atmosphere in which to work, and for providing a substantial amount of computing time without which the numerical method of this work could not have been developed.

I would also like to thank the Natural Sciences and Engineering Research Council of Canada for generous financial support, and Mrs. Helen Kennelly for her excellent typing of the manuscript.

TABLE OF CONTENTS

CHAPTER 1

INTRODUCTION

1.1 Survey

In a classic paper, Slater (1951) analysed the physical implications of the Hartree-Fock equation in order to simplify the troublesome non-local Hartree-Fock exchange potential. As a result of this study, he proposed that the Hartree-Fock exchange potential be approximated by a local potential of the form

$$V_x = - \text{Const} \times \rho^{1/3} . \qquad (1.1)$$

This theory is known as the Hartree-Fock-Slater or $X\alpha$ (see Section 2.3) approximation.

Although the exchange potential (1.1) enjoyed considerable popularity in solid-state calculations, its application to molecular problems was not seriously considered until some two decades later. This delay was due to the successful implementation in atomic and molecular systems of the analytic Hartree-Fock method of Roothaan (1951) which dominated quantum chemical calculations thereafter.

Slater (1965), however, suggested that the exchange potential (1.1) and the so-called "muffin-tin" approximation (Slater 1937) used in solid-state theory might be usefully

combined in order to simplify Hartree-Fock calculations for larger molecular systems. In response to this suggestion, Johnson (1966), modifying the KKR computational scheme of Korringa (1947) and Kohn and Rostoker (1954) for solid-state systems, developed the so-called "Scattered-Wave" or "Multiple-Scattering" scheme for molecular calculations. The theoretical and computational details of this SW-Xα method are nicely reviewed by Slater (1972) and Johnson (1973) respectively.

The SW-Xα method indeed proved to be very computationally efficient, and a considerable number of calculations on a large variety of systems soon appeared. A good review of these early applications of the method is given by Johnson (1975).

Although the SW-Xα scheme was devised particularly for larger molecular systems, it has also been applied to very simple molecules for testing purposes. In addition to the references cited by Johnson (1975), we note, for example, the recent calculations on the diatomics N_2, O_2 and F_2 by Rosenkrantz and Konowalow (1979). These tests indicate that the original SW-Xα muffin-tin model provides reasonable one-electron properties such as transition or ionization energies (Johnson 1975, pg. 44), but that it gives rather poor molecular binding energy curves. In the case of N_2, for example, Rosenkrantz and Konowalow (1979) obtain only 27% of the experimental ground state dissociation energy, and overestimate the bond length by a factor of 1.78.

The classic example of the shortcomings of the standard muffin-tin model is the C_2 molecule, which is actually unbound in the SW-Xα calculations. Non-muffin-tin corrections, however, were investigated by Danese and Connolly (1974), Danese (1974) and Danese (1977) using a perturbative approach which produced remarkably improved binding energy curves. This perturbative procedure, however, is inconvenient for larger systems and much simpler improvements to the muffin-tin scheme were therefore sought.

A straightforward extension of the muffin-tin model to the case of overlapping spheres was suggested by Rosch, Klemperer and Johnson (1973) and by Herman, Williams and Johnson (1974), and was applied to the diatomics N_2, F_2 and CO by Salahub, Messmer and Johnson (1976). These groups obtained significant improvements over the standard touching sphere results, but some uncertainty remains over the choice of appropriate sphere radii.

Also, the scattered-wave or multiple-scattering formalism has been generalized by Williams (1974) to the case of arbitrary cellular partitionings of molecular space, with the inclusion of non-spherical components, but calculations with the theory would appear to involve severe complications. Simpler cellular methods have been proposed by Costas and Garritz (1979), Brescansin, Leite and Ferreira (1979) and Keller (1975) among others.

An interesting variation of the standard muffin-tin

method was introduced by Anderson and Woolley (1973) and was then tested on an extensive series of first row diatomic molecules by Gunnarsson, Harris, and Jones (1977). This Linear Combination of Muffin-Tin Orbitals (LCMTO) method gave vastly improved molecular dissociation energies and bond lengths while retaining the basic simplicity of the muffin-tin model.

Meanwhile, LCAO (Linear Combination of Atomic Orbitals) methods for the solution of the Hartree-Fock-Slater equation were also developed in which muffin-tin or other cellular constructions were discarded altogether. In the so-called Discrete Variational Method (DVM) of Ellis and Painter (1970), molecular orbitals and densities are expanded in a Slater type basis set and the resulting molecular integrals are evaluated numerically using a randomly generated set of integration points and associated weights. The method was refined and applied to various molecular systems in a series of papers by Baerends, Ellis and Ros (1973), Baerends and Ros (1973 and 1975), Heijser, van Kessel and Baerends (1976) and Baerends and Ros (1978). In the last of these papers, the results of test calculations on a series of first row diatomic molecules were presented which showed excellent agreement with experiment, in sharp contrast with the early muffin-tin calculations.

In addition, a GTO-LCAO-Xα method employing Gaussian type basis sets was developed by Sambe and Felton (1975) and further refined by Dunlap, Connolly and Sabin (1979). This method was also tested on a series of first row diatomic mole-

cules, and again the results showed excellent agreement with experiment, but differed somewhat from the results of Baerends and Ros (1978).

This great variety of computational methods (and there are many more which have not been discussed here) has, unfortunately, yielded an equally great variety of results for the dissociation energies, bond lengths, vibrational frequencies and dipole moments of first row diatomic systems. At the present time, therefore, it is very difficult to assess the Hartree-Fock-Slater theory in the presence of the overwhelming numerical error of the existing Xα calculations.

1.2 The Present Work

The LCMTO, DVM and GTO-Xα calculations of Gunnarsson, Harris andJones (1977), Baerends and Ros (1978) and Dunlap, Connolly and Sabin (1979) respectively, are probably the most accurate Hartree-Fock-Slater calculations to date. Even so, the results of these studies show significant discrepancies, despite the tremendous improvement over the early muffin-tin results (see Tables 6.3 to 6.6 in Section 6.3).

In the present work, therefore, a completely "numerical" method for the calculation of diatomic molecular wave functions has been developed in order to provide a reliable assessment of the Hartree-Fock-Slater theory. The method involves the computation of molecular functions at a very large number (i.e. several hundred) of discrete "mesh" points in coordinate space.

We shall make no muffin-tin, cellular, or finite LCAO basis set approximations of any kind. In principle, therefore, the numerical error in these calculations can be virtually eliminated by using a sufficiently large number of mesh points, and this has indeed been accomplished within reasonable tolerances in the present work (see Section 6.2).

Accurate numerical solutions of the Hartree-Fock-Slater equation have, of course, long been available for atomic systems in the form of discrete calculations on a radial mesh. Such calculations culminated in the classic work of Herman and Skillman (1963).

In diatomic systems, however, numerical calculations are somewhat more difficult due to the two-dimensionality of the problem, and therefore very few attempts at such calculations appear in the literature. Gunnarsson and Johansson (1976) used a straightforward numerical approach to test various density functional theories on the simple molecules H_2, H_2^+, He_2 and He_2^{++}. They did not, however, apply their method to more complicated systems.

A remarkably accurate "semi-numerical" method, however, has been developed by McCullough Jr. (1974 and 1975) and Christiansen and McCullough Jr. (1977) for diatomic Hartree-Fock calculations, but this approach has not been applied to Hartree-Fock-Slater or other density functional theories.

Therefore, we have developed in the present work an accurate, completely numerical code for the implementation of

Hartree-Fock-Slater or any other density functional theory to diatomic molecules comprised of arbitrary first row atoms.

The outline of this thesis is as follows: In Chapter 2 a very brief theoretical discussion of the Hartree-Fock-Slater approximation is given. This discussion is not intended to be exhaustive (as the major emphasis of this work is numerical), but it should provide a simple understanding of the theory for the reader who may not be familiar with it.

In Chapter 3 the prolate spheroidal coordinate system for diatomic molecules is introduced and then modified for numerical convenience. We then establish the basic numerical framework for our calculations by defining the discrete mesh used in this work and the corresponding discrete differentiation and integration procedures. This framework is applied in Chapter 4 to the discrete solution of the Hartree-Fock-Slater equation for the molecular orbitals.

In Chapter 5 a somewhat different method for solution of the Poisson equation is presented which has certain advantages in this case over the coordinate space approach of Chapter 4.

Finally, in Chapter 6, the results of extensive calculations on the first row molecules B_2, C_2, N_2, CO, O_2 and F_2 are presented and compared with experiment and also with the results of Gunnarsson, Harris and Jones (1977), Baerends and Ros (1978) and Dunlap, Connolly and Sabin (1979). We assess

these results and the Hartree-Fock-Slater theory in the concluding section of the chapter.

Before we proceed, however, note that all subsequent expressions, unless otherwise specified, are written in atomic units such that $\hbar = e = m_e = 1$.

CHAPTER 2

THE HARTREE-FOCK-SLATER APPROXIMATION

2.1 Hartree-Fock Exchange Energy

In the Hartree-Fock approximation, the wave function for a system of N electrons is represented by an antisymmetrized product of N orthonormal one-electron orbitals ψ_i. If a single such product, or "Slater determinant", is used to calculate the expectation value of the Hamiltonian

$$H = \sum_i \left[-\frac{1}{2} \nabla_i^2 + V_{ext}^{(i)} \right] + \frac{1}{2} \sum_{i \neq j} \frac{1}{r_{ij}} \tag{2.1}$$

then the resulting energy E is given by the expression

$$E = \frac{1}{2} \sum_i \int |\nabla \psi_i|^2 dv + \int V_{ext} \rho dv + \frac{1}{2} \iint \frac{\rho(1)\rho(2)}{r_{12}} dv_1 dv_2 + E_x \tag{2.2}$$

where V_{ext} is the "external" potential arising from the atomic nuclei, ρ is the total electron density

$$\rho = \sum_i |\psi_i|^2 \tag{2.3}$$

and the last term E_x is known as the Hartree-Fock exchange

energy. The exchange energy is the object of the present chapter, and is given by the well known expression

$$E_x = -\frac{1}{2}\sum_{ij}\iint \frac{1}{r_{12}}\psi_i^*(1)\psi_j^*(2)\psi_j(1)\psi_i(2)dv_1dv_2 \ . \qquad (2.4)$$

Details of the derivation are omitted here, since the Hartree-Fock approximation is thoroughly treated in many standard textbooks (see, for example, Tinkham 1964, ch. 6).

In equation (2.4) it is understood that the integration operators and the orbitals ψ_i include spin coordinates. Therefore, it is clear by inspection that the exchange energy consists of two distinct terms, one for each component of spin:

$$E_x = E_{x\uparrow} + E_{x\downarrow} \ . \qquad (2.5)$$

Each term is given by expression (2.4) with the double summation restricted to spin-up and spin-down orbitals respectively. We shall now examine the spin-up exchange energy $E_{x\uparrow}$ in some detail, where, of course, the spin-down term is given by completely analogous formulae.

Notice, first of all, that the exchange energy may be written in the somewhat simpler form

$$E_{x\uparrow} = -\frac{1}{2}\iint \frac{1}{r_{12}}|\rho\uparrow(1,2)|^2 dv_1dv_2 \qquad (2.6)$$

where

$$\rho\uparrow(1,2) = \sum_{i\uparrow} \psi^{*}_{i\uparrow}(1)\psi_{i\uparrow}(2) \quad . \tag{2.7}$$

The function $\rho\uparrow(1,2)$ is called the spin-up one-body density matrix for a Slater determinant. Such density matrices have several useful properties, among which we note that

$$\rho\uparrow(1,1) = \rho\uparrow(1) \tag{2.8}$$

$$\rho\uparrow(2,1) = \rho\uparrow(1,2)^{*} \tag{2.9}$$

and

$$\int \rho\uparrow(1,2)\rho\uparrow(2,3)dv_2 = \rho\uparrow(1,3) \tag{2.10}$$

where the idempotency (2.10) follows from the orthogonality of the orbitals ψ_i. Other interesting properties also exist but shall not concern us here. We will, however, make good use of (2.8-10) shortly.

First, however, the integrand of expression (2.6) may be multiplied and divided by $\rho\uparrow(1)$ to obtain

$$E_{x\uparrow} = -\frac{1}{2}\iint \frac{\rho\uparrow(1)}{r_{12}}\rho_{x\uparrow}(1,2)dv_1dv_2 \tag{2.11}$$

where

$$\rho_{x\uparrow}(1,2) = \frac{|\rho\uparrow(1,2)|^2}{\rho\uparrow(1)} \quad . \tag{2.12}$$

This particular format permits an interesting physical interpretation (Slater 1951) :

Expression (2.11) represents the interaction energy between the spin-up charge density $\rho\uparrow$ and an exchange density $\rho_{x\uparrow}$ defined by (2.12). The general characteristics of this exchange density are determined by the density matrix properties (2.8-10). Using (2.8), the behaviour at $r_2 = r_1$ is given by

$$\rho_{x\uparrow}(1,1) = \rho\uparrow(1) \ . \tag{2.13}$$

Then, using (2.9) and (2.10) the integral of the exchange density is easily seen to be

$$\int \rho_{x\uparrow}(1,2)dv_2 = 1 \ . \tag{2.14}$$

Therefore, the exchange charge density contains exactly one electron, the significance of which will be evident momentarily.

If expression (2.11) is substituted into expression (2.2) for the total energy E, then we obtain

$$\begin{aligned} E = \frac{1}{2}\sum_i \int |\nabla\psi_i|^2 dv + \int V_{ext}\rho dv \\ + \frac{1}{2}\iint \frac{\rho\uparrow(1)}{r_{12}}\,[\rho(2)-\rho_{x\uparrow}(1,2)]dv_1dv_2 \\ + \frac{1}{2}\iint \frac{\rho\downarrow(1)}{r_{12}}\,[\rho(2)-\rho_{x\downarrow}(1,2)]dv_1dv_2 \ . \end{aligned} \tag{2.15}$$

Each of the last two terms represents the interaction energy between the spin-up (or down) charge density and the total charge density minus a so-called "Fermi hole" created by the exchange term. According to equation (2.14) this Fermi hole contains exactly one electron, and consequently each electron in the system actually interacts with a charge density containing only (N-1) electrons. This is physically consistent with the fact that a particle cannot interact with itself, and, therefore, the role of the Hartree-Fock exchange energy is, in part, to cancel the electron self-interaction energy.

2.2 Exchange Energy Approximations

The physical interpretation of the Hartree-Fock exchange energy outlined in the previous section may be used to derive very simple but useful exchange energy approximations. We begin by defining the exchange potential $U_{x\uparrow}$ as the coulomb potential arising from the Fermi hole density:

$$U_{x\uparrow}(1) = - \int \frac{\rho_{x\uparrow}(1,2)}{r_{12}} dv_2 \ . \qquad (2.16)$$

In terms of this definition the exchange energy (2.11) is given by

$$E_{x\uparrow} = \frac{1}{2} \int \rho\uparrow(1) U_{x\uparrow}(1) dv_1 \ . \qquad (2.17)$$

We shall concentrate our efforts in this section on finding an approximate expression for the exchange potential $U_{x\uparrow}$.

Notice, first of all, that calculation of the exchange potential (2.16) does not require a detailed knowledge of the angular dependence of the exchange density. Since the coulomb interaction is spherically symmetric, only the spherical average of $\rho_{x\uparrow}(1,2)$ about the point r_1 is required. We may, therefore, restrict ourselves to spherically symmetric models of the exchange density without loss of generality.

These models must, of course, satisfy the general conditions (2.13) and (2.14) of the previous section. It follows from (2.13) that the value of the exchange density at the centre of our spherical model must be $\rho\uparrow(1)$, and it follows from (2.14) that its integrated value must be unity.

As a first approximation, Slater (1951) models the exchange density with a uniform sphere of constant density $\rho\uparrow$ and radius R. Applying the normalization constraint, we obtain

$$R = \left(\frac{3}{4\pi\rho\uparrow}\right)^{1/3} \qquad (2.18)$$

which provides a rough estimate for the size of the Fermi hole. The resulting exchange potential for this model is easily found to be

$$U_{x\uparrow} = -\ 3.90\ \left(\frac{3}{4\pi}\ \rho\uparrow\right)^{1/3} . \qquad (2.19)$$

Although obviously crude, this model probably reflects the gross behaviour of the exchange potential fairly well.

A more realistic approximation might involve the use of a Gaussian model having the form

$$\rho_{x\uparrow}(s) = \rho\uparrow e^{-as^2} \tag{2.20}$$

where the parameter "a" is determined by the normalization condition. We choose a Gaussian rather than an exponential model in order to avoid the introduction of a cusp at the origin . After some straightforward algebra, the following exchange potential is obtained:

$$U_{x\uparrow} = - 3.22 \left(\frac{3}{4\pi} \rho\uparrow\right)^{1/3} \tag{2.21}$$

which has the same form as the previous approximation (2.19) with a slightly different coefficient.

In fact, on purely dimensional grounds, Slater (1974, pg. 34) stresses that <u>any</u> such one-parameter model for the spherically averaged exchange density will yield a potential which is proportional to $\rho^{1/3}$. Therefore, we conclude that the Hartree-Fock exchange potential can be approximated by an expression of the form

$$U_{x\uparrow} = - C_x \rho\uparrow^{1/3} \tag{2.22}$$

where, for historical reasons discussed in the next section, the constant C_x is conventionally written in the form

$$C_x = \frac{9}{2} \alpha \left(\frac{3}{4\pi}\right)^{1/3} . \tag{2.23}$$

For the uniform sphere and Gaussian models which we have considered, the values of the parameter α are 0.87 and 0.72 res-

pectively. Obviously, it is necessary to determine an "optimum" value for α in some reasonable manner, but we shall postpone the discussion of this problem until the next section.

Recall that the Hartree-Fock exchange energy is given by expression (2.17). Substituting the approximate exchange potential (2.22) into this expression, we obtain

$$E_{x\uparrow} = -\frac{1}{2} C_x \int \rho\uparrow^{4/3} dv \tag{2.24}$$

which is certainly very much simpler than the original expression (2.4).

The approximation (2.24) is the desired result of the present section, but its usefulness can only be assessed by experience with calculations on "real" atomic and molecular systems.

2.3 The Xα Method

The exchange energy approximation (2.24) and its spin-down counterpart, when substituted into expression (2.2) for the total energy, give

$$\begin{aligned} E = & \frac{1}{2} \sum_i \int |\nabla \psi_i|^2 dv + \int V_{ext} \rho dv \\ & + \frac{1}{2} \iint \frac{\rho(1)\rho(2)}{r_{12}} dv_1 dv_2 \\ & - \frac{1}{2} C_x \int (\rho\uparrow^{4/3} + \rho\downarrow^{4/3}) dv \end{aligned} \tag{2.25}$$

where the constant C_x is given by equation (2.23) of the previous section.

We now assume that the orbitals ψ_i may be determined by the usual variational procedure applied, in this case, to the approximate energy (2.25). Minimizing (2.25) with respect to the orbitals ψ_i produces an equation for the orbitals containing an exchange potential V_x arising from the last term. This potential V_x should not be confused with the potential U_x of the previous section, as they have entirely different meanings.

Since the spin-up and the spin-down electron densities are generally not equal, the exchange potential V_x is, in fact, spin dependent. For simplicity, however, it is preferable to work with spin restricted orbitals, and we therefore introduce a non-spin-polarized approximation for the energy (2.25) by replacing $\rho\uparrow$ and $\rho\downarrow$ with $\rho/2$. We obtain

$$\begin{aligned} &E(\text{non-spin-polarized}) \\ &= \frac{1}{2}\sum_i \int |\nabla\psi_i|^2 dv + \int V_{ext}\rho dv \\ &+ \frac{1}{2}\iint \frac{\rho(1)\rho(2)}{r_{12}} dv_1 dv_2 \\ &- C_x \int (\rho/2)^{4/3} dv \ . \end{aligned} \tag{2.26}$$

Of course, this expression is equal to the energy (2.25) in cases where the electrons are, in fact, completely spin paired.

Equating the variation of expression (2.26) with respect to variations in the orbital ψ_k to zero, we obtain the following equation for the spin restricted orbitals of the system :

$$-\frac{1}{2}\nabla^2\psi_k + (V_{ext}+V_{el}+V_x)\psi_k = \varepsilon_k\psi_k \qquad (2.27)$$

where V_{el} is the coulomb potential arising from the total electron density:

$$V_{el}(1) = \int \frac{\rho(2)}{r_{12}}\, dv_2 \qquad (2.28)$$

and the exchange potential V_x is given by

$$V_x = -3\alpha\left(\frac{3}{8\pi}\rho\right)^{1/3} . \qquad (2.29)$$

Equation (2.27) must, of course, be solved in an iterative and self-consistent manner, since the electron density itself appears in the potentials V_{el} and V_x.

Note that, although the orbitals are assumed to be spin restricted in this work, the total energy E is calculated using the properly spin-polarized expression (2.25).

Equation (2.27) and the local exchange potential (2.29) were suggested by Slater in 1951 in order to simplify Hartree-Fock calculations for solid-state systems. Therefore, the present theory is often referred to as the Hartree-Fock-Slater

approximation. Slater's original approach is somewhat different from that which we have taken here, and the interested reader is advised to consult Slater's 1951 paper for further details.

However, Gaspar (1954) and then Kohn and Sham (1965) argued that Slater's exchange potential was too large, and that a coefficient having two thirds of Slater's value was more appropriate. This uncertainty has prompted workers in the field to define the coefficient in terms of an adjustable parameter called "α" (see expression (2.23)) such that $\alpha = 1$ and $\alpha = 2/3$ correspond to the Slater and the Gaspar-Kohn-Sham potentials respectively. The term "Xα" is commonly applied to this parameterized version of the Hartree-Fock-Slater theory.

Several studies have been undertaken to determine the optimum value for α empirically, the best known of these being a study of atomic systems by Schwarz (1972). He solved the Xα equation (2.27) for a large number of atoms and determined the optimum α for each atom by choosing the value which gave an Xα total energy (2.25) equal to the Hartree-Fock energy. The resulting empirical α's lie between 0.7 and 0.8, depending on the atom.

Theoretical studies have also been made in order to account for the empirical results. We note, for example, the work of Gopinathan, Whitehead and Bogdanovic (1976) and Gasquez and Keller (1977).

For molecular systems, however, the choice of α is somewhat less clear. In the diatomic calculations of Gunnarsson,

Harris and Jones (1977), Baerends and Ros (1978) and Dunlap, Connolly and Sabin (1979) a "uniform α" approximation with $\alpha = 0.7$ was used. For compatibility with the work of these groups, therefore, the same approximation has been applied to the present calculations.

Although many interesting aspects of the theory have not been considered here, we shall now conclude this brief discussion of the Hartree-Fock-Slater approximation and refer the reader to an excellent review by Slater (1974) for further details.

CHAPTER 3

THE COORDINATE SYSTEM

3.1 Prolate Spheroidal Coordinates

In this chapter, a convenient and efficient coordinate system is constructed to serve as a framework for numerical calculations on diatomic systems.

Of the several standard two-centre orthogonal coordinate systems available, the prolate spheroidal coordinates (see, for example, Arfken 1970, pg. 103) are the most suitable starting point for our purposes. The orthogonal surfaces of this system consist of confocal ellipsoids and hyperboloids of revolution. Assuming that the focal points are located at (0,0,-a) and (0,0,a), the transformation equations are

$$x = a \sinh\epsilon_1 \sin\epsilon_2 \cos\phi \qquad (3.1a)$$

$$y = a \sinh\epsilon_1 \sin\epsilon_2 \sin\phi \qquad (3.1b)$$

$$z = a \cosh\epsilon_1 \cos\epsilon_2 \qquad (3.1c)$$

where coordinates ϵ_1 and ϵ_2 label the ellipsoidal and hyperboloidal surfaces respectively, and ϕ is the azimuth angle. A representative sketch of this coordinate system is given in Figure 3.1.

Figure 3.1

Prolate Spheroidal Coordinates ε_1 and ε_2.

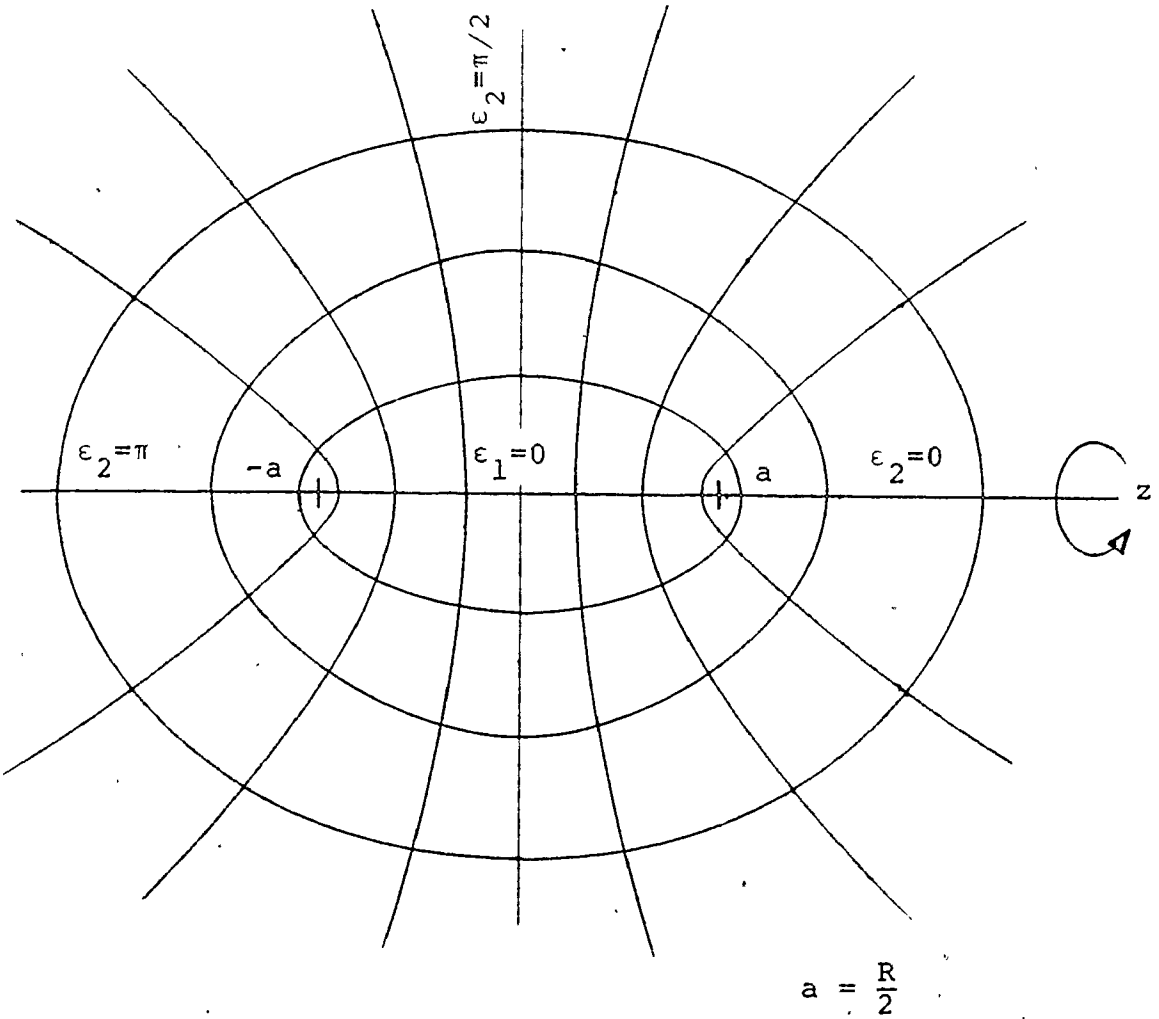

The domains of these coordinates are

$$0 \leq \varepsilon_1 < \infty \tag{3.2a}$$

$$0 \leq \varepsilon_2 \leq \pi \tag{3.2b}$$

and, of course,

$$0 \leq \phi \leq 2\pi \ . \tag{3.2c}$$

In the case of an axially symmetric system, the ϕ dependence of our molecular orbitals can be handled analytically, and therefore the problem is simply two-dimensional.

Let the focal points (0,0,-a) and (0,0,a) be denoted centre 1 and centre 2 respectively. Then the distance from centre 1 to a given point (x,y,z) is denoted r_1, and the distance from centre 2 is denoted r_2. In terms of the prolate spheroidal coordinates, these distances are given by

$$r_1 = a(\cosh\varepsilon_1 + \cos\varepsilon_2) \tag{3.3a}$$

$$r_2 = a(\cosh\varepsilon_1 - \cos\varepsilon_2) \ . \tag{3.3b}$$

These expressions immediately reveal an interesting property of the prolate spheroidal system, namely that exponential functions of r_1 or r_2 transform into Gaussian functions of ε_1 and ε_2 near the nuclei. In the $(\varepsilon_1,\varepsilon_2)$ coordinate system there are no nuclear cusps.

Finally, for future reference, the scale factors and the volume element for this coordinate system are given below: (see Arfken 1970, ch. 2, for a discussion of the scale factors

h_i of a curvilinear coordinate system.)

$$h_1 = h_2 = (r_1 r_2)^{1/2} \tag{3.4a}$$

$$h_\phi = a \sinh\varepsilon_1 \sin\varepsilon_2 \tag{3.4b}$$

and

$$dv = a r_1 r_2 \sinh\varepsilon_1 \sin\varepsilon_2 d\varepsilon_1 d\varepsilon_2 d\phi \ . \tag{3.5}$$

3.2 Transformation from $(\varepsilon_1 \varepsilon_2)$ to $(x_1 x_2)$

It is desirable for numerical purposes to transform from the coordinates ε_1 and ε_2 to a new set of coordinates which we shall call x_1 and x_2. In this way the distribution of ε_1 and ε_2 coordinate surfaces in real space can be optimized to improve numerical accuracy. Furthermore, the semi-infinite domain of the ε_1 coordinate can be transformed into a finite domain.

We begin by seeking a transformation of the form $\varepsilon_1(x_1)$ which has the following properties:

$$0 \leq x_1 \leq 1 \tag{3.6}$$

and

$$\varepsilon_1(0) = 0 \tag{3.7a}$$

$$\varepsilon_1(\tfrac{1}{2}) = \varepsilon_{1m} \tag{3.7b}$$

$$\varepsilon_1(1) = \infty \tag{3.7c}$$

where ε_{1m} labels the ellipsoid corresponding to the midpoint of the x_1 domain. In addition, we require that ε_1 be an odd

function of x_1 in order to facilitate the application of boundary conditions at $x_1 = 0$, as discussed in the next section.

A suitable transformation is given by

$$\varepsilon_1 = c_1 \tanh^{-1}(x_1) = \frac{1}{2} c_1 \ln\left(\frac{1+x_1}{1-x_1}\right) \tag{3.8a}$$

where

$$c_1 = \frac{2\varepsilon_{1m}}{\ln 3} . \tag{3.8b}$$

Of course, the choice (3.8) is not unique, but investigation of its asymptotic behaviour indicates that this transformation is appropriate for our problem. We discuss this matter in Appendix A.

The purpose of parameter ε_{1m}, defined by equation (3.7b), is to scale the distribution of the ellipsoidal surfaces to an appropriate atomic size. If we let r_m denote the "size" of the atoms comprising the molecule, then ε_{1m} is defined in the present work as the ellipsoid with semi-major axis $(a+r_m)$. This definition gives

$$\varepsilon_{1m} = \cosh^{-1}\left(1 + \frac{r_m}{a}\right) . \tag{3.9}$$

Furthermore, for the two-shell atoms considered in this work, the atomic "size" r_m is defined as the radius corresponding to the minimum of the charge distribution $r^2\rho(r)$ between the shells. Then, in the case of a heteronuclear molecule, we define r_m as the geometric mean of the constituent atomic values.

Through the transformation $\varepsilon_1(x_1)$, therefore, the semi-infinite domain of ε_1 has been mapped onto the finite domain of x_1, and the distribution of ellipsoids in real space has been optimized through the parameter ε_{1m}.

Although the second coordinate ε_2 already spans a finite domain, it is desirable to introduce a second transformation $\varepsilon_2(x_2)$ in order to adjust the real space distribution of the hyperbolic surfaces as well. A suitable transformation for this purpose is given by

$$\varepsilon_2 = x_2 + c_2 \sin 2x_2 \tag{3.10a}$$

where

$$0 \leq x_2 \leq \pi \tag{3.10b}$$

and

$$-\frac{1}{2} < c_2 < \frac{1}{2} . \tag{3.10c}$$

For negative values of c_2, the transformation (3.10) increases the concentration of hyperboloids near the foci, and conversely, for positive values of c_2 the concentration of hyperboloids near the foci is reduced. Therefore, depending on the degree of concentration of the molecular density near the nuclei, proper adjustment of this parameter can improve numerical accuracy somewhat.

Since the domain of possible values for c_2 is restricted by (3.10c), its optimum value has been determined in the present work by trial calculations using very coarse meshes. These trials indicate that the value $c_2 = -0.25$ is appropriate

for the first row molecules considered in this work.

In principle, of course, the precise values of the constants c_1 (or ε_{1m}) and c_2 are irrelevant if a sufficiently large number of mesh points is used, but proper choice of these constants often allows a significant reduction in the number of mesh points required to achieve a given computational accuracy.

In summary, then, the original prolate spheroidal coordinates $\varepsilon_1\varepsilon_2$ have now been replaced by coordinates x_1x_2, and our problem is therefore defined on a finite rectangle in x_1x_2-space. This rectangle is illustrated in Figure 3.2, where we also give the physical significance of its boundaries. In the following section we shall discuss the boundary conditions applicable to molecular functions on the perimeter of this region.

3.3 Boundary Conditions

It is clear from the original transformation equations (3.1) that the coordinate values $\varepsilon_1 = 0$, $\varepsilon_2 = 0$ and $\varepsilon_2 = \pi$ correspond to the nuclear axis of the system. In this section we examine what happens when the values of the coordinates ε_1 and ε_2 are extended beyond these boundaries.

First of all, equations (3.1) imply that any given point (x,y,z) is transformed into the point (-x,-y,z) under

a sign change in either ε_1 or ε_2. A similar transformation is also affected by a change in the value of ε_2 from $(\pi-\delta)$ to $(\pi+\delta)$ for some arbitrary δ.

Therefore, when the values of the coordinates ε_1 and ε_2 are extended across the boundaries $\varepsilon_1 = 0$, $\varepsilon_2 = 0$ and $\varepsilon_2 = \pi$, this corresponds to a perpendicular crossing of the axis in real space.

Notice, furthermore, that the coordinate transformations $\varepsilon_1(x_1)$ and $\varepsilon_2(x_2)$ of the previous section are designed to preserve these properties. A sign change in x_1 or x_2, or a change in the value of x_2 from $(\pi-\delta)$ to $(\pi+\delta)$ all result in the transformation of an arbitrary point (x,y,z) into the point $(-x,-y,z)$. Consequently, the boundary conditions applicable to a given molecular function at $x_1 = 0$, $x_2 = 0$ and $x_2 = \pi$ are related to its <u>axial symmetry</u>.

For clarity, these boundary conditions will now be precisely stated for functions of σ and π symmetry, which are the only symmetries of concern to us in the present work: with x_2 constant, a $\sigma(\pi)$ function must be even (odd) about the point $x_1 = 0$, and similarly, with x_1 constant, a $\sigma(\pi)$ function must be even (odd) about the points $x_2 = 0$ and $x_2 = \pi$. In addition, it is also interesting to note that all molecular functions are actually periodic in x_2 (for x_1 constant) with a period of 2π, although this information is not utilized in the present calculations.

Figure 3.2

The x_1 x_2 Coordinate System.

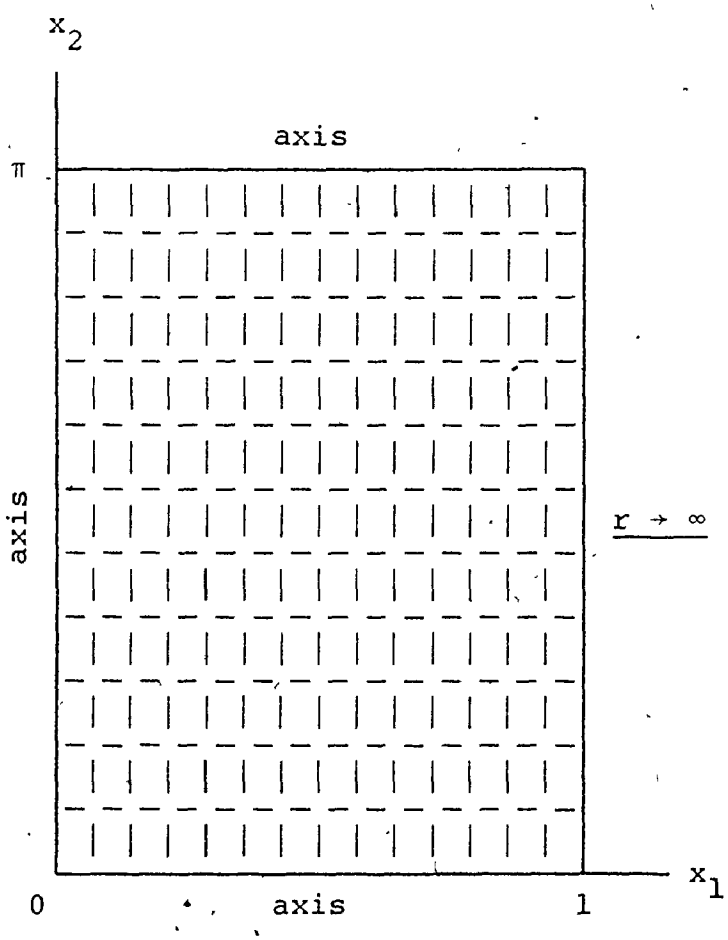

We have not, as yet, mentioned the boundary at $x_1 = 1$, which corresponds to the ellipsoid at infinity. In the present work, we simply constrain all functions and their normal first derivative to vanish along this boundary.

Before concluding this section, the homonuclear molecule deserves special consideration. In this case, of course, only half of the normal range of the x_2 coordinate is needed (i.e. $0 \leq x_2 \leq \pi/2$) and at the boundary $x_2 = \pi/2$ a given function must be either even or odd (for x_1 constant) depending on the reflection symmetry of the state in question. At all other boundaries the previous conditions are obviously unchanged.

3.4 Discretization

Our problem is defined in the rectangle

$$0 \leq x_1 \leq 1 \tag{3.11a}$$

$$0 \leq x_2 \leq \pi \tag{3.11b}$$

with boundary conditions as discussed in the previous section. Let us now discretize the problem by constructing a uniform two-dimensional mesh on this rectangle containing, say, $N_1 \times N_2$ points. Since the coordinate system is orthogonal, this mesh is simply a product of two independent one-dimensional meshes for each of the x_1 and x_2 components.

As discussed in Section 4.2, all functions dealt with in this work (i.e. σ functions included) actually vanish on the boundaries of the rectangle (3.11), and therefore no mesh points

are required on the perimeter. The x_1 mesh, therefore, contains N_1 points excluding $x_1 = 0$ and $x_1 = 1$, and the x_2 mesh contains N_2 points excluding $x_2 = 0$ and $x_2 = \pi$. The coordinates of the mesh point designated ij are simply

$$x_1 = ih_1 \quad , \quad x_2 = jh_2 \tag{3.12}$$

where

$$h_1 = 1/(N_1+1) \quad , \quad h_2 = \pi/(N_2+1) \ . \tag{3.13}$$

In the subsequent work, we adopt the convention that indices i and j refer to the x_1 and the x_2 meshes respectively.

In the case of a homonuclear molecule, of course, only half of the normal x_2 mesh is required. Notice, however, that two different kinds of half-meshes exist, depending on whether the original full mesh contains an even or an odd number of points. It can be shown that the former case is preferable, and in Figure 3.3 this half-mesh is illustrated, along with the full meshes for both the x_1 and the x_2 coordinates.

Having described the structure of the x_1 and the x_2 meshes, we now proceed to a discussion of discrete analogs for differentiation and integration operators.

Corresponding to partial differentiation operators, we shall define two matrices on the mesh which generate approximate partial derivatives of an arbitrary function F at any given mesh point ij.

Figure 3.3

Form of the x_1 and the x_2 Meshes.

$\underline{x_1}$ Mesh:

$\underline{x_2}$ Mesh (Heteronuclear Molecule):

$\underline{x_2}$ Mesh (Homonuclear Molecule):

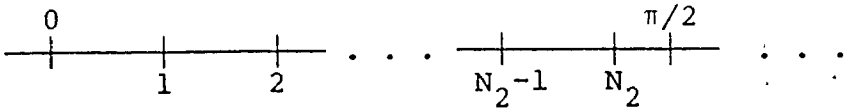

For partial differentiation with respect to x_1, we define the $N_1 \times N_1$ matrix $d^{(1)}$ such that

$$\left.\frac{\partial F}{\partial x_1}\right|_{ij} \simeq \sum_{k=1}^{N_1} d^{(1)}_{ik} F_{kj} , \qquad (3.14)$$

and similarly, for partial differentiation with respect to x_2, we define the $N_2 \times N_2$ matrix $d^{(2)}$ such that

$$\left.\frac{\partial F}{\partial x_2}\right|_{ij} \simeq \sum_{k=1}^{N_2} d^{(2)}_{jk} F_{ik} . \qquad (3.15)$$

These matrices incorporate the appropriate boundary conditions of the previous section, and therefore a distinct matrix is required for each distinct set of boundary conditions (i.e. for each symmetry class).

In the present work, $d^{(1)}$ and $d^{(2)}$ have been calculated using cubic spline analysis, but any desired numerical technique can be used. The cubic spline derivation is outlined in Appendix B.

It is also possible, in principle, to define matrices which generate higher order derivatives, but the variational formalism of the next chapter requires first order derivatives only.

The cubic spline analysis of Appendix B also produces a set of integration weights for each of the x_1 and x_2 meshes.

These weights, designated $w_i^{(1)}$ and $w_j^{(2)}$, are defined by

$$\int F(x_1)dx_1 \approx \sum_i w_i^{(1)} F_i \tag{3.16a}$$

$$\int F(x_2)dx_2 \approx \sum_j w_j^{(2)} F_j \,. \tag{3.16b}$$

Two-dimensional integrations are performed by combining these expressions in the usual manner:

$$\iint F(x_1,x_2)dx_1dx_2 = \sum_{ij} w_i^{(1)} w_j^{(2)} F_{ij} \,. \tag{3.17}$$

This equation gives approximate integrals in x_1x_2-space, but let us proceed further and derive a simple integration formula for volume integrations in "real" space.

Consider the volume integration over all space of an arbitrary axially symmetric function F. In order to eliminate a factor $(2\pi a)$ from all subsequent expressions, it is convenient to redefine the integration weights $w_i^{(1)}$ and $w_j^{(2)}$ as follows:

$$\begin{aligned} w_i^{(1)} &\to (2\pi a)^{1/2} w_i^{(1)} \\ w_j^{(2)} &\to (2\pi a)^{1/2} w_j^{(2)} \,. \end{aligned} \tag{3.18}$$

Then, using expression (3.5) for the volume element in prolate

spheroidal coordinates and equation (3.17) for integrations in x_1x_2-space, we obtain the following expression for the volume integral of the function F:

$$\iiint F dv \simeq \sum_{ij} w_{ij} F_{ij} \qquad (3.19a)$$

where the volume integration weights w_{ij} are given by

$$w_{ij} = w_i^{(1)} w_j^{(2)} (r_1 r_2 \sinh\epsilon_1 \sin\epsilon_2 \frac{d\epsilon_1}{dx_1} \frac{d\epsilon_2}{dx_2})_{ij} . \qquad (3.19b)$$

This discrete integration formula will be used on many occasions throughout the remainder of this work.

CHAPTER 4

DISCRETE SOLUTION OF THE HARTREE-FOCK-SLATER EQUATION

4.1 The Variational Formulation

Recall that the Hartree-Fock-Slater (or Xα) orbitals satisfy an equation of the form

$$-\frac{1}{2}\nabla^2\psi_k + V\psi_k = \varepsilon_k\psi_k \tag{4.1}$$

where the self-consistent potential V is given by

$$V = V_{ext} + V_{el} + V_x \tag{4.2}$$

(see equations (2.27-29)). It is possible to replace this equation by an equivalent matrix problem by directly substituting for the differential operators in (4.1) the discrete differentiation matrices described in Section 3.4. The resulting problem, however, is non-symmetric and therefore this direct approach is not recommended.

It is well known, however, that equation (4.1) can be recast as a variational problem in which we seek the extrema of the functional

$$F = \frac{1}{2}\int |\nabla\psi|^2 dv + \int (V-\varepsilon)|\psi|^2 dv \ . \tag{4.3}$$

We can treat this variational problem by replacing the functional F with a discrete approximation using the numerical machinery of Section 3.4. Then, equating to zero the variation in F with respect to the value of ψ at each of the mesh points, we ultimately generate an equivalent matrix problem which is, in this case, symmetric. This symmetry follows from the symmetric positive definite form of the kinetic energy integral used in expression (4.3).

Notice, also, that the variational formulation does not require the evaluation of any derivatives higher than first order, which is numerically very convenient.

Therefore, the discrete variational approach outlined above has been used in the present work for calculating molecular orbitals. In the sections that follow, we describe the application of this method first of all to orbitals of σ symmetry, and then to orbitals of π symmetry.

4.2 σ Orbitals

For notational convenience in this and the following section, let us define the integrals T and I_v as follows:

$$T = \int |\nabla\psi|^2 dv \qquad (4.4)$$

$$I_v = \int (V-\varepsilon)|\psi|^2 dv \ . \qquad (4.5)$$

In terms of these definitions, of course, the functional F

is simply

$$F = \frac{1}{2} T + I_v \ . \qquad (4.6)$$

In this section, simple discrete approximations for the integrals T and I_v will be discussed for orbitals of σ symmetry.

Notice, first of all, that σ orbitals have non-zero value along the internuclear axis, but that the prolate spheroidal volume element (3.5) vanishes there. Unfortunately, this implies that the variational formalism of the previous section cannot directly provide σ orbital values along the axis. Therefore, we define a new function

$$\mu = (\sinh\varepsilon_1 \sin\varepsilon_2)\psi \qquad (4.7)$$

which is the simplest conceivable modification of ψ that vanishes on the axis. This function vanishes asymptotically as well, if the behaviour of ψ is exponential.

Regarding Sections 3.3 and 3.4 of the previous chapter, we note that the function μ has zero value along the entire perimeter of the rectangle (3.11), and that it has π axial symmetry.

Let us return now to a discussion of the integral T, expression (4.4). Using the prolate spheroidal scale factors (3.4) the integrand of T may be written as

$$|\nabla\psi|^2 = \frac{1}{r_1 r_2} \left[\left(\frac{\partial\psi}{\partial\varepsilon_1}\right)^2 + \left(\frac{\partial\psi}{\partial\varepsilon_2}\right)^2 \right] \qquad (4.8)$$

which is conveniently separated into two terms:

$$T = T_1 + T_2 \tag{4.9}$$

where

$$T_1 = \int \left(\frac{\partial \psi}{\partial \varepsilon_1}\right)^2 \frac{dv}{r_1 r_2} \tag{4.10a}$$

$$T_2 = \int \left(\frac{\partial \psi}{\partial \varepsilon_2}\right)^2 \frac{dv}{r_1 r_2} \quad . \tag{4.10b}$$

The treatments of these two terms are very similar, and we therefore need consider only T_1 in detail.

In terms of the function μ defined by (4.7), we have

$$T_1 = \int \left(\frac{\partial \mu}{\partial \varepsilon_1} - \frac{\cosh \varepsilon_1}{\sinh \varepsilon_1}\,\mu\right)^2 \frac{dv}{r_1 r_2 \sinh^2 \varepsilon_1 \sin^2 \varepsilon_2} \tag{4.11}$$

which, after changing the variable of differentiation ε_1 to x_1, and then applying the discrete integration formula (3.19) becomes

$$T_1 = \sum_{ij} \frac{w_i^{(1)} w_j^{(2)}}{\sinh \varepsilon_1 \sin \varepsilon_2} \left(\frac{d\varepsilon_1}{dx_1}\right)\left(\frac{d\varepsilon_2}{dx_2}\right)\left(\frac{dx_1}{d\varepsilon_1}\frac{\partial \mu}{\partial x_1} - \frac{\cosh \varepsilon_1}{\sinh \varepsilon_1}\,\mu\right)^2_{ij} \quad . \tag{4.12}$$

This expression can be simplified considerably, as we now proceed to do.

We begin with the definition of new weights $\omega_{\sigma i}^{(1)}$ and $\omega_{\sigma j}^{(2)}$, given by

$$\omega_{\sigma i}^{(1)} = \frac{w_i^{(1)}}{\sinh\varepsilon_1} \left(\frac{d\varepsilon_1}{dx_1}\right) \tag{4.13a}$$

$$\omega_{\sigma j}^{(2)} = \frac{w_j^{(2)}}{\sin\varepsilon_2} \left(\frac{d\varepsilon_2}{dx_2}\right) \tag{4.13b}$$

where the index σ is used in order to distinguish these from analogous weights defined for π orbitals in the next section.

Then, we introduce the $N_1 \times N_1$ matrix $D_\sigma^{(1)}$ defined by the following equation:

$$\left(\frac{dx_1}{d\varepsilon_1}\frac{\partial\mu}{\partial x_1} - \frac{\cosh\varepsilon_1}{\sinh\varepsilon_1}\mu\right)_{ij} = \sum_k D_{\sigma ik}^{(1)}\mu_{kj} \,. \tag{4.14}$$

In terms of the differentiation matrix $d^{(1)}$ of Section 3.4 this definition gives

$$D_{\sigma ii'}^{(1)} = \left(\frac{dx_1}{d\varepsilon_1}\right)_i d_{ii'}^{(1)} - \left(\frac{\cosh\varepsilon_1}{\sinh\varepsilon_1}\right)_i \delta_{ii'} \,. \tag{4.15}$$

Substituting the definitions (4.13) and (4.14) into (4.12), we obtain the simplified expression

$$T_1 = \sum_{ij} \omega_{\sigma i}^{(1)}\omega_{\sigma j}^{(2)} \left(\sum_k D_{\sigma ik}^{(1)}\mu_{kj}\right)^2 \tag{4.16}$$

which can be rewritten as

$$T_1 = \sum_{ijk\ell} \omega_{\sigma i}^{(1)}\omega_{\sigma j}^{(2)} D_{\sigma ik}^{(1)} D_{\sigma i\ell}^{(1)} \mu_{kj}\mu_{\ell j} \,. \tag{4.17}$$

This expression can be further simplified by performing the summation over index i, which results in the definition

of a symmetric $N_1 \times N_1$ matrix $A_\sigma^{(1)}$ given by

$$A_{\sigma k\ell}^{(1)} = \sum_i \omega_{\sigma i}^{(1)} D_{\sigma ik}^{(1)} D_{\sigma i\ell}^{(1)} \tag{4.18}$$

in terms of which the integral T_1 may be written in the following final form:

$$T_1 = \sum_{jk\ell} \omega_{\sigma j}^{(2)} A_{\sigma k\ell}^{(1)} \mu_{kj} \mu_{\ell j} \ . \tag{4.19}$$

This result is a very convenient discrete approximation for the original expression (4.10a).

Completely analogous results exist for the second integral T_2, expression (4.10b), and these are summarized below:

$$T_2 = \sum_{ik\ell} \omega_{\sigma i}^{(1)} A_{\sigma k\ell}^{(2)} \mu_{ik} \mu_{i\ell} \tag{4.20}$$

where $\omega_{\sigma i}^{(1)}$ is given by (4.13a), and the $N_2 \times N_2$ matrix $A_\sigma^{(2)}$ is defined by

$$A_{\sigma k\ell}^{(2)} = \sum_j \omega_{\sigma j}^{(2)} D_{\sigma jk}^{(2)} D_{\sigma j\ell}^{(2)} \tag{4.21}$$

with $\omega_{\sigma j}^{(2)}$ given by (4.13b), and the $N_2 \times N_2$ matrix $D_\sigma^{(2)}$ related to $d^{(2)}$ of Section 3.4 by

$$D_{\sigma jj'}^{(2)} = \left(\frac{dx_2}{d\varepsilon_2}\right)_j d_{jj'}^{(2)} - \left(\frac{\cos\varepsilon_2}{\sin\varepsilon_2}\right)_j \delta_{jj'} \ . \tag{4.22}$$

Notice that the matrix $A_\sigma^{(2)}$, similarly to $A_\sigma^{(1)}$, is symmetric.

Having considered the kinetic energy integral T, we now turn to a discussion of the integral I_v given by expression (4.5). Recalling definition (4.7) of the function μ and then applying the discrete integration formula (3.19), we immediately write

$$I_v = \sum_{ij} \omega_{ij}(V-\varepsilon)\mu_{ij}^2 \tag{4.23}$$

where the weights ω_{ij} are defined by

$$\omega_{ij} = \frac{w_{ij}}{\sinh^2\varepsilon_1 \sin^2\varepsilon_2} . \tag{4.24}$$

Expression (4.23) is the discrete analog of the original integral (4.5).

Let us now calculate the variations of expressions (4.19), (4.20) and (4.23) for T_1, T_2 and I_v respectively with respect to a variation in the value of μ at the mesh point IJ. Using the obvious relation

$$\frac{\partial \mu_{ij}}{\partial \mu_{IJ}} = \delta_{iI}\delta_{jJ} \tag{4.25}$$

the following results are easily obtained:

$$\frac{\partial T_1}{\partial \mu_{IJ}} = 2\omega_{\sigma J}^{(2)} \sum_i A_{\sigma Ii}^{(1)} \mu_{iJ} \tag{4.26a}$$

$$\frac{\partial T_2}{\partial \mu_{IJ}} = 2\omega_{\sigma I}^{(1)} \sum_j \mu_{Ij} A_{\sigma jJ}^{(2)} \tag{4.26b}$$

and

$$\frac{\partial I_V}{\partial \mu_{IJ}} = 2\omega_{IJ}(V_{IJ}-\varepsilon)\mu_{IJ} \cdot \tag{4.27}$$

Then, equating the variation of the functional F, expression (4.6), to zero using the above results, we finally obtain the following set of equations (one for each mesh point IJ) for the discrete values of μ:

$$\frac{\omega^{(2)}_{\sigma J}}{2} \sum_i A^{(1)}_{\sigma Ii}\mu_{iJ} + \frac{\omega^{(1)}_{\sigma I}}{2} \sum_j \mu_{Ij}A^{(2)}_{\sigma jJ} + \omega_{IJ}V_{IJ}\mu_{IJ}$$

$$= \varepsilon\omega_{IJ}\mu_{IJ} \cdot \tag{4.28}$$

The set of equations (4.28) constitutes an equivalent matrix representation of the original differential Hartree-Fock-Slater equation (4.1). Before discussing the method of solution, however, we must also consider orbitals of π symmetry for which a similar set of equations is derived in the following section.

4.3 π Orbitals

An orbital of π symmetry can be written in the form

$$\psi = \mu e^{\pm i\phi} \tag{4.29}$$

where μ is a two-dimensional function of ε_1 and ε_2 which vanishes along the internuclear axis. Therefore, the transformation (4.7) is not required in this case.

As in the previous section, we shall here discuss discrete approximations for the integrals T and I_v defined by expressions (4.4) and (4.5) respectively. Beginning with the integral T, we use the scale factors (3.4) to obtain

$$|\nabla\psi|^2 = \frac{1}{r_1 r_2}\left[\left(\frac{\partial\mu}{\partial\varepsilon_1}\right)^2 + \left(\frac{\partial\mu}{\partial\varepsilon_2}\right)^2\right] + \frac{\mu^2}{a^2\sinh^2\varepsilon_1\sin^2\varepsilon_2} . \tag{4.30}$$

Therefore, the integral T for π orbitals is composed of three terms,

$$T = T_1+T_2+T_3 \tag{4.31}$$

where

$$T_1 = \int \left(\frac{\partial\mu}{\partial\varepsilon_1}\right)^2 \frac{dv}{r_1 r_2} \tag{4.32a}$$

$$T_2 = \int \left(\frac{\partial\mu}{\partial\varepsilon_2}\right)^2 \frac{dv}{r_1 r_2} \tag{4.32b}$$

and

$$T_3 = \frac{1}{a^2}\int \frac{\mu^2 dv}{\sinh^2\varepsilon_1\sin^2\varepsilon_2} . \tag{4.33}$$

The treatment of the terms T_1 and T_2 closely parallels the discussion of the previous section, but differences arise due to the absence of transformation (4.7) in this case. Omitting details then, the new results are summarized in the following paragraph.

Again, we begin by defining new weights $\omega_{\pi i}^{(1)}$ and $\omega_{\pi j}^{(2)}$ given, in this case, by

$$\omega_{\pi i}^{(1)} = w_i^{(1)} \sinh\epsilon_1 \left(\frac{d\epsilon_1}{dx_1}\right) \tag{4.34a}$$

$$\omega_{\pi j}^{(2)} = w_j^{(2)} \sin\epsilon_2 \left(\frac{d\epsilon_2}{dx_2}\right) . \tag{4.34b}$$

Then, we define the $N_1 \times N_1$ matrix $D_\pi^{(1)}$ and the $N_2 \times N_2$ matrix $D_\pi^{(2)}$ as follows:

$$D_{\pi ii'}^{(1)} = \left(\frac{dx_1}{d\epsilon_1}\right)_i d_{ii'}^{(1)} \tag{4.35a}$$

$$D_{\pi jj'}^{(2)} = \left(\frac{dx_2}{d\epsilon_2}\right)_j d_{jj'}^{(2)} \tag{4.35b}$$

where $d^{(1)}$ and $d^{(2)}$ are the differentiation matrices of Section 3.4. From these are constructed the symmetric $N_1 \times N_1$ and $N_2 \times N_2$ matrices $A_\pi^{(1)}$ and $A_\pi^{(2)}$ given by

$$A_{\pi k\ell}^{(1)} = \sum_i \omega_{\pi i}^{(1)} D_{\pi ik}^{(1)} D_{\pi i\ell}^{(1)} \tag{4.36a}$$

$$A_{\pi k\ell}^{(2)} = \sum_j \omega_{\pi j}^{(2)} D_{\pi jk}^{(2)} D_{\pi j\ell}^{(2)} \tag{4.36b}$$

in terms of which the integrals T_1 and T_2 are finally written as

$$T_1 = \sum_{jk\ell} \omega_{\pi j}^{(2)} A_{\pi k\ell}^{(1)} \mu_{kj} \mu_{\ell j} \tag{4.37a}$$

$$T_2 = \sum_{ik\ell} \omega_{\pi i}^{(1)} A_{\pi k\ell}^{(2)} \mu_{ik} \mu_{i\ell} . \tag{4.37b}$$

These expressions have the same form as (4.19) and (4.20) of the previous section.

Let us now consider the third kinetic energy term T_3 given by expression (4.33). Applying the discrete integration formula (3.19) and recalling the definition (4.24) of the weights ω_{ij} in the previous section, we easily obtain

$$T_3 = \frac{1}{a^2} \sum_{ij} \omega_{ij} \mu_{ij}^2 \quad . \tag{4.38}$$

And finally, for the integral I_v defined by expression (4.5), the discrete integration formula (3.19) immediately gives

$$I_v = \sum_{ij} w_{ij} (V-\varepsilon) \mu_{ij}^2 \quad . \tag{4.39}$$

Since the expressions for T_1, T_2 and I_v of the present section have forms similar to those of the previous section, we may re-apply the equations (4.26) and (4.27) in order to calculate variations with respect to the value of μ at the mesh point IJ. Using, in addition, the obvious result

$$\frac{\partial T_3}{\partial \mu_{IJ}} = \frac{2}{a^2} \omega_{IJ} \mu_{IJ} \tag{4.40}$$

and equating to zero the variation of the functional F, expression (4.6), we obtain the following set of equations (one for each mesh point IJ) for the discrete values of μ:

$$\frac{\omega_{\pi J}^{(2)}}{2} \sum_i A_{\pi Ii}^{(1)} \mu_{iJ} + \frac{\omega_{\pi I}^{(1)}}{2} \sum_j \mu_{Ij} A_{\pi jJ}^{(2)} + \frac{\omega_{IJ}}{2a^2} \mu_{IJ}$$

$$+ w_{IJ} V_{IJ} \mu_{IJ} = \varepsilon w_{IJ} \mu_{IJ} . \qquad (4.41)$$

These equations for discrete π orbitals have the same form as equations (4.28) for σ orbitals, with the exception of an extra term arising from the integral T_3. We shall discuss their solution in the following section.

4.4 The Equivalent Matrix Problem

The results of the previous two sections are summarized below:

$$\frac{\omega_{\lambda J}^{(2)}}{2} \sum_i A_{\lambda Ii}^{(1)} \mu_{iJ} + \frac{\omega_{\lambda I}^{(1)}}{2} \sum_j \mu_{Ij} A_{\lambda jJ}^{(2)} + \theta_{\lambda IJ} \mu_{IJ}$$

$$+ \Omega_{\lambda IJ} V_{IJ} \mu_{IJ} = \varepsilon \Omega_{\lambda IJ} \mu_{IJ} \qquad (4.42)$$

where λ is a symmetry index indicating either σ or π symmetry, and

for σ orbitals $\qquad \psi = \frac{\mu}{\sinh\varepsilon_1 \sin\varepsilon_2}$ (4.42a)

$$\theta_{\sigma IJ} = 0 \qquad (4.42b)$$

$$\Omega_{\sigma IJ} = \omega_{IJ} \qquad (4.42c)$$

and similarly,

for π orbitals $$\psi = \mu e^{\pm i\phi} \tag{4.42d}$$

$$\theta_{\pi IJ} = \frac{\omega_{IJ}}{2a^2} \tag{4.42e}$$

$$\Omega_{\pi IJ} = w_{IJ} \ . \tag{4.42f}$$

The set of equations (4.42) is equivalent to a matrix problem of order $N = N_1 \times N_2$, and we discuss this problem in the present section.

Until now, the discrete mesh points described in Section 3.4 have been labelled by the pair of subscripts i and j, but it is also possible to order these points into a singly subscripted array by defining the following index k:

$$k = (j-1)N_1 + i \ . \tag{4.43}$$

Using this indexing scheme, the discrete array of μ values is considered to be one-dimensional, and by inspection we see that equations (4.42) are equivalent to a generalized matrix eigenvalue problem of the form

$$A\mu = \varepsilon B\mu \tag{4.44}$$

where the N×N matrix A is symmetric, and the matrix B is diagonal.

It is clear from the form of equations (4.42) that the matrix A has a simple and well defined block structure, which, rather than attempting a written description, is illustrated in

Figure 4.1 for the case of a 5×6 point mesh. This particular structure is, of course, a consequence of the fact that we are working in an orthogonal coordinate system. Notice that the matrix is extremely sparse (i.e. mostly zeros).

The matrix equation (4.44) is, however, complicated by the appearance of the "metric" B on the right hand side. Since the elements of B are all positive, though, equation (4.44) is very easily transformed into standard form. We begin by defining the square root matrix

$$R = B^{1/2} \tag{4.45}$$

and substituting this definition into (4.44), we obtain

$$R^{-1}A\mu = \varepsilon R\mu \ . \tag{4.46}$$

If we now define the new vector

$$x = R\mu \tag{4.47}$$

then equation (4.46) can be written in the standard form

$$(R^{-1}AR^{-1})x = \varepsilon x \tag{4.48}$$

where the matrix $(R^{-1}AR^{-1})$ is, of course, still symmetric. This equation may now be solved using one of the many available algorithms for symmetric eigenvalue problems.

In the present work, it is wise to exploit the fact that matrix A is very sparse, and the fact that good approximations for the orbitals of the system exist at the outset of

each self-consistent iteration. These factors are both exploited by iterative numerical matrix methods, and for this work the so-called Lanczos algorithm has been chosen. Rather than digress at this point, we discuss the Lanczos algorithm in Appendix C.

Figure 4.1

Structure of the Matrix A , equation (4.44)

$N_1 = 5$

$N_2 = 6$

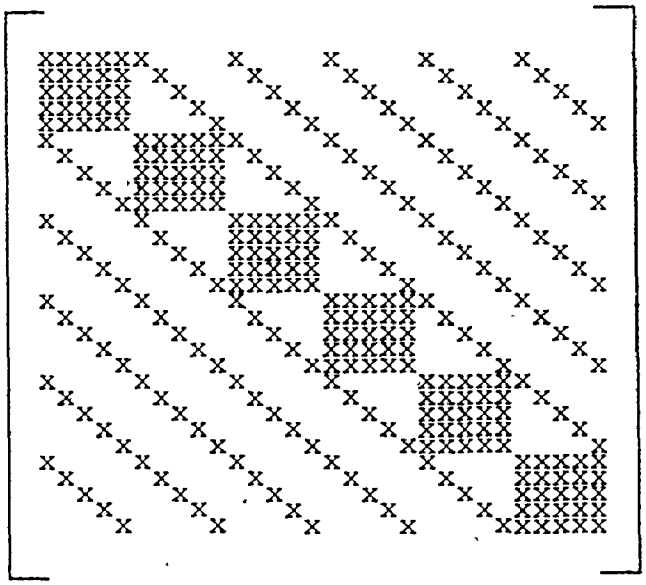

CHAPTER 5

THE POISSON EQUATION

5.1 Coordinate Space Representation

The self-consistent potential (4.2) contains a term V_{el} which is the coulomb potential arising from the total electron density. Although this potential is defined by the integral (2.28), it is much more convenient to determine V_{el} by solving the Poisson equation

$$\nabla^2 V_{el} = -4\pi\rho \tag{5.1}$$

where ρ is the total electron density (2.3). As discussed in Section 4.1 in connection with the Hartree-Fock-Slater equation, the Poisson equation (5.1) can be discretized by direct substitution of the differentiation matrices of Section 3.4. Again, however, the resulting matrix problem is non-symmetric, and therefore this approach is undesirable.

Consequently, as in the previous chapter, we recast equation (5.1) as a variational problem and this formulation generates an equivalent matrix equation which is symmetric and positive definite.

The Poisson equation is equivalent to minimization of the functional

$$F = \frac{1}{2}\int (\nabla V_{el})^2 dv - 4\pi \int \rho V_{el} dv \ . \qquad (5.2)$$

Since the first term of this functional is similar to the first term of functional (4.3) of the previous chapter, and since V_{el} has σ symmetry, we may apply the results of Section 4.2 directly to the present case. Defining

$$\mu = (\sinh\varepsilon_1 \sin\varepsilon_2) V_{el} \qquad (5.3)$$

we obtain the following set of equations for the coulomb potential:

$$\omega^{(2)}_{\sigma J} \sum_i A^{(1)}_{\sigma Ii}\mu_{iJ} + \omega^{(1)}_{\sigma I} \sum_j \mu_{Ij} A^{(2)}_{\sigma jJ} = 4\pi\omega_{IJ}(\sinh\varepsilon_1 \sin\varepsilon_2 \rho)_{IJ} \qquad (5.4)$$

where the right hand side arises from the second term of the functional (5.2).

If μ is considered to be a one-dimensional array under the indexing scheme (4.43), then the set of equations (5.4) is equivalent to a matrix equation of the form

$$A\mu = b \qquad (5.5)$$

where matrix A has the structure previously illustrated in Figure 4.1. Furthermore, recalling definitions (4.18) and (4.21) of the matrices $A^{(1)}_\sigma$ and $A^{(2)}_\sigma$ respectively, we also note that A is symmetric and positive definite.

Since the matrix A is sparse, and since a good approximation for the coulomb potential is always available in self-consistent calculations, equation (5.5) may be solved using any of a number of well known iterative numerical algorithms. Specially designed for symmetric positive definite systems, for example, is the method of Conjugate Gradients outlined by Schwarz (1973, ch. 2).

In the present work, however, the Poisson equation has been solved much more efficiently by employing a cubic B-spline rather than a coordinate space representation. We discuss this approach in the following section.

5.2 The Cubic B-Spline Representation

Suppose that we have a set of basis functions $\phi_i^{(1)}$ which span x_1 space, and also a basis set $\phi_j^{(2)}$ which spans x_2 space. Two-dimensional functions $\mu(x_1 x_2)$ can then be written as linear combinations of the form

$$\mu = \sum_{ij} a_{ij} \phi_i^{(1)} \phi_j^{(2)} . \qquad (5.6)$$

If the first derivatives of the basis functions are denoted $\theta_i^{(1)}$ and $\theta_j^{(2)}$, then we also have

$$\frac{\partial \mu}{\partial x_1} = \sum_{ij} a_{ij} \theta_i^{(1)} \phi_j^{(2)} \qquad (5.7a)$$

$$\frac{\partial \mu}{\partial x_2} = \sum_{ij} a_{ij} \phi_i^{(1)} \theta_j^{(2)} . \qquad (5.7b)$$

If the x_1 and x_2 coordinates are discretized, we define matrices $\phi^{(1)}_{ii'}$, $\phi^{(2)}_{jj'}$, $\theta^{(1)}_{ii'}$ and $\theta^{(2)}_{jj'}$ such that, for example, $\phi^{(1)}_{ii'}$ denotes the value of $\phi^{(1)}_i$ at the mesh point i'. We then write

$$\mu_{IJ} = \sum_{ij} a_{ij} \phi^{(1)}_{iI} \phi^{(2)}_{jJ} \tag{5.8}$$

and similar expressions for the partial derivatives (5.7).

Now let us use this representation to approximate the functional F given by expression (5.2). We begin by defining the integrals

$$T = \int (\nabla V_{el})^2 dv \tag{5.9}$$

$$I_\rho = 4\pi \int \rho V_{el} dv \tag{5.10}$$

such that

$$F = \frac{1}{2} T - I_\rho \tag{5.11}$$

The integral T, as in Section 4.2, can be written as the sum of two terms T_1 and T_2. Concentrating for the moment on the first of these terms, we recall expressions (4.12) and (4.13) in order to write

$$T_1 = \sum_{rs} \omega^{(1)}_{\sigma r} \omega^{(2)}_{\sigma s} \left(\frac{dx_1}{d\epsilon_1} \frac{\partial \mu}{\partial x_1} - \frac{\cosh \epsilon_1}{\sinh \epsilon_1} \mu \right)^2_{rs} . \tag{5.12}$$

This expression can be simplified by defining the matrix

$$\Omega_{ir}^{(1)} = \left(\frac{dx_1}{d\varepsilon_1}\right)_r \theta_{ir}^{(1)} - \left(\frac{\cosh\varepsilon_1}{\sinh\varepsilon_1}\right)_r \phi_{ir}^{(1)} \tag{5.13}$$

which, when substituted into expression (5.12) gives

$$\begin{aligned} T_1 &= \sum_{rs} \omega_{\sigma r}^{(1)} \omega_{\sigma s}^{(2)} \left[\sum_{ij} a_{ij} \Omega_{ir}^{(1)} \phi_{js}^{(2)}\right]^2 \\ &= \sum_{rs} \sum_{ij} \sum_{i'j'} \omega_{\sigma r}^{(1)} \omega_{\sigma s}^{(2)} a_{ij} a_{i'j'} \Omega_{ir}^{(1)} \Omega_{i'r}^{(1)} \phi_{js}^{(2)} \phi_{j's}^{(2)} . \end{aligned} \tag{5.14}$$

Then, performing the summations over indices r and s, we construct the symmetric positive definite matrices $D^{(1)}$ and $B^{(2)}$ given by

$$D_{ii'}^{(1)} = \sum_r \omega_{\sigma r}^{(1)} \Omega_{ir}^{(1)} \Omega_{i'r}^{(1)} \tag{5.15a}$$

$$B_{jj'}^{(2)} = \sum_s \omega_{\sigma s}^{(2)} \phi_{js}^{(2)} \phi_{j's}^{(2)} \tag{5.15b}$$

in terms of which the integral T_1 is written in the simple form

$$T_1 = \sum_{ij} \sum_{i'j'} a_{ij} a_{i'j'} D_{ii'}^{(1)} B_{jj'}^{(2)} . \tag{5.16}$$

Similarly, the second term T_2 of the integral (5.9) can be written in the same form:

$$T_2 = \sum_{ij} \sum_{i'j'} a_{ij} a_{i'j'} B_{ii'}^{(1)} D_{jj'}^{(2)} \tag{5.17}$$

where the matrices $B^{(1)}$ and $D^{(2)}$ are defined by

$$B^{(1)}_{ii'} = \sum_r \omega^{(1)}_{\sigma r} \phi^{(1)}_{ir} \phi^{(1)}_{i'r} \tag{5.18a}$$

$$D^{(2)}_{jj'} = \sum_s \omega^{(2)}_{\sigma s} \Omega^{(2)}_{js} \Omega^{(2)}_{j's} \tag{5.18b}$$

and the matrix $\Omega^{(2)}$ is given by

$$\Omega^{(2)}_{js} = \left(\frac{dx_2}{d\varepsilon_2}\right)_s \theta^{(2)}_{js} - \left(\frac{\cos\varepsilon_2}{\sin\varepsilon_2}\right)_s \phi^{(2)}_{js} . \tag{5.19}$$

Notice again that the matrices $B^{(1)}$ and $D^{(2)}$, given by (5.18), are symmetric and positive definite.

Combining the expressions (5.16) and (5.17) for T_1 and T_2 respectively, we finally obtain the following discrete approximation for the integral T, equation (5.9):

$$T = \sum_{ij} \sum_{i'j'} a_{ij} a_{i'j'} [D^{(1)}_{ii'} B^{(2)}_{jj'} + B^{(1)}_{ii'} D^{(2)}_{jj'}] . \tag{5.20}$$

The variation of this expression with respect to a variation in the coefficient a_{IJ} is simply

$$\frac{\partial T}{\partial a_{IJ}} = 2 \sum_{ij} a_{ij} [D^{(1)}_{iI} B^{(2)}_{jJ} + B^{(1)}_{iI} D^{(2)}_{jJ}] \tag{5.21}$$

where the obvious relation $\partial a_{ij}/\partial a_{IJ} = \delta_{iI}\delta_{jJ}$ has been used to derive this result.

Let us now consider the second term I_ρ of the functional F, given by expression (5.10). Applying the discrete integration formula (3.19) and the definition (5.3) we write

$$I_\rho = 4\pi \sum_{rs} \omega_{rs} (\sinh\varepsilon_1 \sin\varepsilon_2 \rho)_{rs} \mu_{rs} \tag{5.22}$$

where the weights ω_{rs} are defined by (4.24) of the previous chapter. Employing the basis set representation (5.8) this becomes

$$I_\rho = 4\pi \sum_{rs} \sum_{ij} a_{ij}\omega_{rs}(\sinh\varepsilon_1 \sin\varepsilon_2\rho)_{rs}\phi^{(1)}_{ir}\phi^{(2)}_{js} \qquad (5.23)$$

and the variation of this expression with respect to a_{IJ} is clearly

$$\frac{\partial I_\rho}{\partial a_{IJ}} = 4\pi \sum_{rs} \omega_{rs}(\sinh\varepsilon_1 \sin\varepsilon_2\rho)_{rs}\phi^{(1)}_{Ir}\phi^{(2)}_{Js} \ . \qquad (5.24)$$

Finally, equating the variation of F, expression (5.11), to zero using (5.21) and (5.24), we obtain the following set of equations (one for each IJ) for the expansion coefficients a_{ij}:

$$\sum_{ij} a_{ij}[B^{(1)}_{iI}D^{(2)}_{jJ} + D^{(1)}_{iI}B^{(2)}_{jJ}]$$

$$= 4\pi \sum_{rs} \omega_{rs}(\sinh\varepsilon_1 \sin\varepsilon_2\rho)_{rs}\phi^{(1)}_{Ir}\phi^{(2)}_{Js} \ . \qquad (5.25)$$

After solving this set of equations for the a_{ij}, the function values μ_{ij} are obtained from (5.8) and then the coulomb potential V_{el} from definition (5.3).

Incorporating the now familiar re-indexing scheme (4.43), the set of equations (5.25) is seen to be equivalent to a matrix equation of the form

$$Ax = b \qquad (5.26)$$

where x is the column vector of coefficients a_k, and the matrix A is symmetric and positive definite.

The structure of A is determined by the structure of the matrices $B^{(1)}$, $B^{(2)}$, $D^{(1)}$ and $D^{(2)}$ defined by expressions (5.15) and (5.18). In general, these matrices are full, and therefore the solution of (5.26) is hopelessly difficult for a typical number of basis functions (i.e. several hundred).

In Appendix D, however, we discuss a class of basis functions on a uniform discrete mesh known as B-splines, which are characterized by the fact that they are maximally localized subject to certain continuity constraints. These functions are therefore ideal for our purposes, because the basis matrices $\phi^{(1)}_{ii'}$ and $\phi^{(2)}_{jj'}$ are banded. In fact, for the special case of cubic B-splines, these basis matrices are tridiagonal, as shown in Appendix E.

If the basis matrices are tridiagonal, then the matrices $B^{(1)}$, $B^{(2)}$, $D^{(1)}$ and $D^{(2)}$ are, from expressions (5.15) and (5.18), quindiagonal, which simplifies the matrix problem (5.26) tremendously. By inspection of (5.25) we see that matrix A becomes block quindiagonal with a detailed structure as illustrated in Figure 5.1 for the special case of a 7×8 point mesh.

Being positive definite and banded, with a relatively small bandwidth, our problem is now easily solved by the method of Cholesky Decomposition (see for example, Fox 1964,

ch. 4) in which we calculate the matrix L and its transpose L^T such that

$$A = LL^T \tag{5.27}$$

where L is a lower triangular band matrix with the same bandwidth as A. The matrix L is stored, and then for any given right hand side b, the linear system (5.26) can be solved in two stages:

$$Ly = b \tag{5.28a}$$

$$L^T x = y \tag{5.28b}$$

where y and x are computed by forward and then backward substitution respectively.

This method is extremely rapid once the Cholesky decomposition has been obtained. Therefore, solution of the Poisson equation demands a very small fraction of overall computer time in the present work.

5.3 Asymptotic Behaviour

For reasons discussed in Section 4.2, we have dealt in this chapter with the function

$$\mu = (\sinh\varepsilon_1 \sin\varepsilon_2) V_{el} \tag{5.29}$$

rather than with V_{el} itself. Asymptotically, however, we notice that the coulomb potential V_{el} behaves like

$$V_{el} \sim r^{-1} \tag{5.30}$$

and we also deduce from equation (3.3) that the factor $\sinh\varepsilon_1$

behaves like

$$(\sinh\varepsilon_1) \sim r \ . \tag{5.31}$$

Therefore, it is obvious that the function μ does not vanish asymptotically, but rather approaches

$$\mu \sim \text{const} \times \sin\varepsilon_2 \ . \tag{5.32}$$

This asymptotic limit introduces complications at the boundary $x_1 = 1$.

Consequently, it is preferable to work with the equation

$$\nabla^2(V_{el}-V_0) = -4\pi(\rho-\rho_0) \tag{5.33}$$

where ρ_0 is some "reference" density with the same total charge as ρ, and V_0 is its coulomb potential. In the present work, for example, ρ_0 is a sum of spherical atomic densities for which V_0 can be calculated analytically.

Since the density difference $(\rho-\rho_0)$ has zero total charge, the asymptotic behaviour of $(V_{el}-V_0)$ is given by

$$(V_{el}-V_0) \sim r^{-2} \tag{5.34}$$

and therefore the function μ <u>does</u>, in this case, vanish asymptotically and simple zero boundary conditions may be applied at $x_1 = 1$. Of course, equation (5.33) is solved in exactly the same manner as the original equation (5.1), and we need not modify the discussion of the previous section in any way.

Figure 5.1

Structure of the Matrix A , equation (5.26)

$N_1 = 7$

$N_2 = 8$

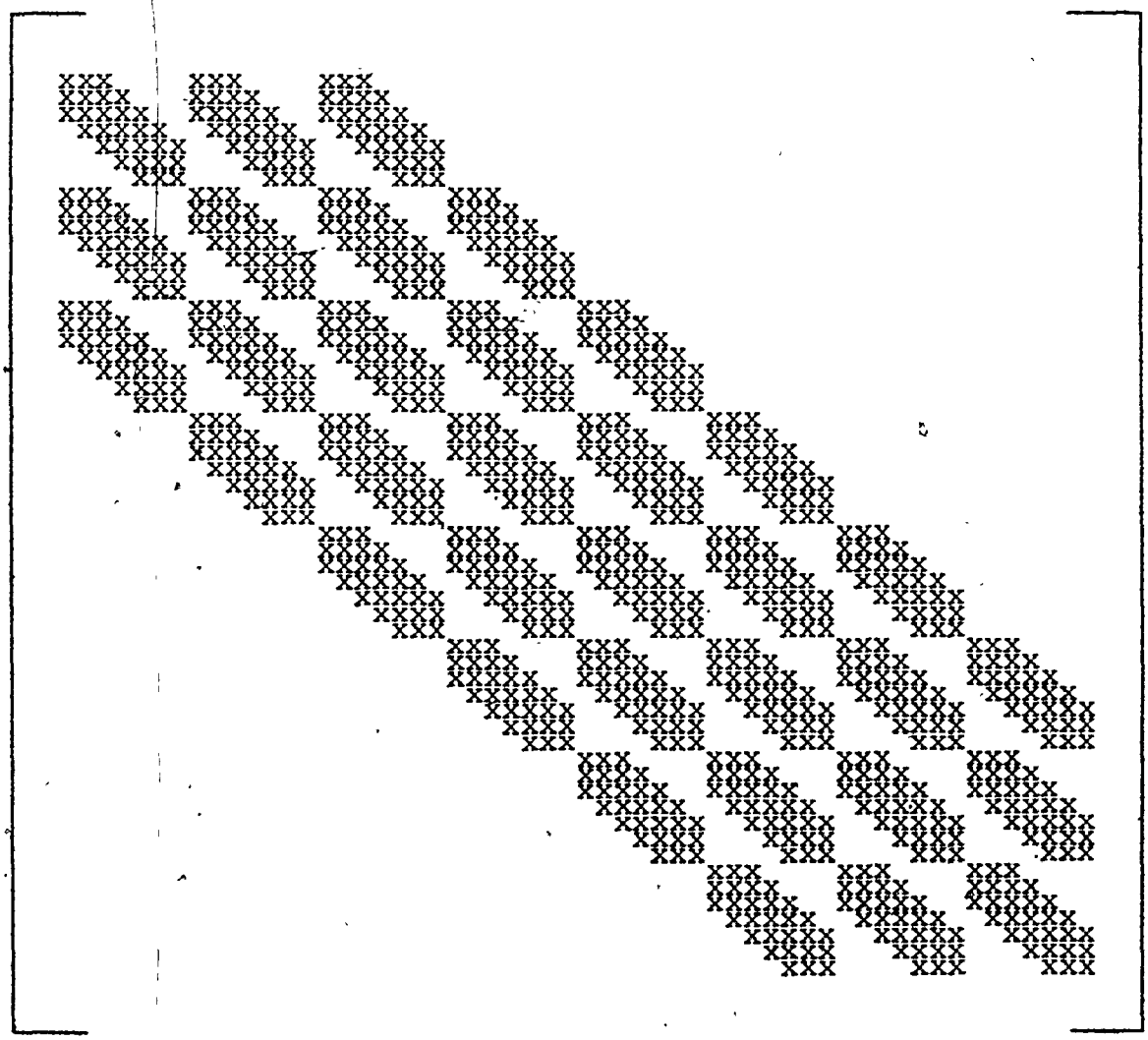

CHAPTER 6

CALCULATIONS

6.1 Outline of the Calculations

The first row homonuclear diatomics B_2, C_2, N_2, O_2 and F_2 as well as the heteronuclear molecule CO have been chosen as tests of the numerical method outlined in the previous chapters and of the Hartree-Fock-Slater theory. For each of these molecules the ground state dissociation energy, bond length, vibrational frequency and quadrupole moment (or dipole moment) have been calculated.

The ground state configurations of these molecules are given below:

B_2	$1\sigma_g^2 1\sigma_u^2 2\sigma_g^2 2\sigma_u^2 1\pi_u^2$	$^3\Sigma_g^-$
C_2	$1\sigma_g^2 1\sigma_u^2 2\sigma_g^2 2\sigma_u^2 1\pi_u^4$	$^1\Sigma_g^+$
N_2	$1\sigma_g^2 1\sigma_u^2 2\sigma_g^2 2\sigma_u^2 3\sigma_g^2 1\pi_u^4$	$^1\Sigma_g^+$
CO	$1\sigma^2 2\sigma^2 3\sigma^2 4\sigma^2 1\pi^4 5\sigma^2$	$^1\Sigma^+$
O_2	$1\sigma_g^2 1\sigma_u^2 2\sigma_g^2 2\sigma_u^2 3\sigma_g^2 1\pi_u^4 1\pi_g^2$	$^3\Sigma_g^-$
F_2	$1\sigma_g^2 1\sigma_u^2 2\sigma_g^2 2\sigma_u^2 3\sigma_g^2 1\pi_u^4 1\pi_g^4$	$^1\Sigma_g^+$

We reiterate that the orbitals used in this work are spin re-

stricted, but that the Xα total energy is calculated in the properly spin polarized form (2.25). This applies, of course, to the open shell ground states of the molecules B_2 and O_2 and also to the ^2P, ^3P, ^4S, ^3P and ^2P ground states of the atoms B, C, N, O and F respectively, used in the calculation of dissociation energies. Note that all of the open shell states considered here are representable by a single Slater determinant, and therefore the simple theory of Chapter 2 is applicable (see, however, Ziegler, Rauk and Baerends (1977) for a simple extension of the theory to certain multideterminantal situations).

Trial calculations on the molecules N_2 and CO indicate that the densities of the atomic 1s core orbitals can be frozen without significantly affecting orbital energies, dissociation energies or molecular charge densities, and therefore the core orbitals have in fact been frozen in the subsequent calculations. Frozen cores are trivially incorporated into the present numerical scheme by explicitly orthogonalizing valence orbitals with respect to the core orbitals as part of the Lanczos reorthogonalization procedure of Appendix C.

Self-consistency has been achieved in the present calculations by mixing the "old" and the "new" potentials of a given cycle in the ratio

$$V_{\text{next cycle}} = \frac{2}{3} V_{\text{old}} + \frac{1}{3} V_{\text{new}} \qquad (6.1)$$

to generate the self-consistent potential for the next cycle. This prescription leads to stable convergence in roughly ten iterations. The potential for the first cycle, of course, is generated from the sum of the constituent atomic densities.

6.2 Mesh Tests

To begin with, calculations have been performed at the experimental equilibrium internuclear separations in order to investigate the sensitivity of our results to the number of mesh points used. These calculations are a stringent test of the numerical accuracy of the present method.

In Table 6.1, ground state dissociation energies for our six test molecules are presented as a function of the number of mesh points used in their calculation. For each molecule, we begin with a 98 point mesh (i.e. 7×14 points), and thereafter the calculation is successively repeated using roughly twice the previous number of points until convergence in the bond energy (to the nearest 0.1 eV) is achieved. This convergence is, in fact, successfully obtained in all cases with 800 mesh points or less.

These dissociation energies have been calculated from the expression

$$D_e = |E_{AB} - E_A - E_B| \qquad (6.2)$$

where the atomic energies E_A and E_B are computed by exactly the same numerical code and on the same discrete mesh as the

corresponding molecular calculation for E_{AB}. This is done, of course, by assigning zero charge to one of the nuclei in the molecular program. In this way, thanks to error cancellation in the difference (6.2), very accurate dissociation energies are obtained even on the coarser meshes despite somewhat larger errors in the absolute energies themselves.

Furthermore, the errors in the absolute energies can be estimated by comparing the atomic energies derived from the present code with accurate atomic results. For this purpose an atomic code which utilizes the extended basis sets of Clementi and Roetti (1974) has been written to provide accurate atomic Xα energies. The comparisons indicate that the absolute error in the total energy on a 98 point mesh is typically in the order of electron volts, whereas the error on the 800 point mesh is less than 0.1 eV.

As a result of these atomic studies and the studies of Table 6.1, we feel that the dissociation energies reported here are accurate to 0.1 eV.

The molecular charge densities have also been investigated as a function of mesh size by calculating quadrupole moments for the homonuclear molecules, and the dipole moment of CO. These moments are presented in Table 6.2, and have been calculated, of course, using the discrete integration formula (3.19). We note that they display satisfactory consistency despite an eightfold overall increase in the number of mesh points.

These calculations show that the present numerical method performs extremely well for the first row molecules considered here. In the following section, we shall compare our results with experiment and also with some recent calculations in the literature.

Table 6.1

Dissociation Energies D_e (eV)

	Number of Mesh Points*			
	7×14	10×20	15×30	20×40
B_2	4.2	3.8	3.8	
C_2	7.0	6.3	6.2	6.2
N_2	9.9	9.7	9.6	9.6
CO	12.4	12.1	12.1	
O_2	7.5	7.2	7.1	7.1
F_2	4.3	3.7	3.3	3.3

*Note: Only half of the indicated number of mesh points are actually needed for the homonuclear calculations, but the full number is required for the corresponding atomic calculations of equation (6.2).

Table 6.2

Quadrupole Moments Q (10^{-26} esu cm^2)

$$Q = \frac{1}{2}\int \rho(3z^2-r^2)\, dv$$

Number of Mesh Points

	7×7	10×10	15×15	20×20
B_2	0.98	1.17	1.15	
C_2	2.88	3.12	3.15	3.24
N_2	-1.84	-1.59	-1.53	-1.55
O_2	-0.61	-0.53	-0.53	-0.48
F_2	0.95	0.94	0.93	0.93

Dipole Moment of CO (10^{-18} esu cm)

$N_1 \times N_2$	$\mu(C^+O^-)$
7×14	-0.25
10×20	-0.26
15×30	-0.24

6.3 Results

As mentioned in Section 2.3, the diatomic Xα calculations of Gunnarsson, Harris and Jones (1977), Baerends and Ros (1978) and Dunlap, Connolly and Sabin (1979) were performed using the uniform value $\alpha = 0.7$. Since these calculations are probably the most accurate Xα calculations to date, the same approximation has been applied to the present work in order that direct comparisons between their results and the present results can be made. For convenience we shall refer to these groups as GHJ, BR and DCS respectively in the remainder of this section.

In Table 6.3, we compare the ground state dissociation energies of the present work with experiment, with the results of GHJ, BR and DCS, and with the results of Hartree-Fock calculations.

Notice, first of all, that the agreement with experiment is remarkably good for such a simple theory, with the largest absolute discrepancy being 1.9 eV for the O_2 molecule. In every case the Xα dissociation energy shows improvement over the Hartree-Fock value, which is well known to underbind molecular systems. The Xα approximation, on the other hand, gives slightly overbound molecules in many cases, which is permitted by the fact that the Xα theory is not a "proper" many-body variational theory (i.e. the total energy is not the expectation value of the many-body Hamiltonian (2.1) for an explicit many-body wave function).

Even more interesting, however, is the excellent agreement (with the possible exception of N_2) between the present results and those of DCS. The previous dissociation energies of GHJ, BR and DCS show significant discrepancies, and therefore this agreement is very gratifying.

We have also calculated the spectroscopic constants r_e and ω_e; the equilibrium internuclear separation and the vibrational frequency. These have been determined by fitting a cubic polynomial in inverse powers of the internuclear separation to seven points in the vicinity of r_e separated by 0.1 bohr. At each of these points the energy difference (6.2) has been computed in order to eliminate small variations in the numerical error of our calculation as a function of the internuclear separation.

The above fitting function and distribution of points have been chosen to correspond with the work of DCS, who point out that the vibrational frequency ω_e is rather sensitive to the exact choice of these factors. Vibrational frequencies from other sources, however, should be comparable within about 50 cm^{-1}.

In Table 6.4 we compare the equilibrium internuclear separations r_e with experiment, with the results of GHJ, BR and DCS, and with Hartree-Fock results, and in Table 6.5 we compare vibrational frequencies ω_e.

Considering, first of all, the bond lengths r_e, we notice that the agreement with experiment is again remarkably

good, with the largest discrepancy being 0.07 bohr for the F_2 molecule. Furthermore, the agreement between the present results and the DCS results is again excellent, with the largest discrepancy in this case being only 0.02 bohr.

These general comments apply to the vibrational frequencies ω_e as well. With the exception of the F_2 molecule, the calculated frequencies lie within 40 cm^{-1} of the experimental values, and similar agreement is also found with the results of DCS. As noted in connection with dissociation energies, the present Hartree-Fock-Slater results are generally preferable to those of the Hartree-Fock theory.

In Table 6.6 we present the calculated dipole moment of the CO molecule and its derivative at the experimental equilibrium internuclear separation along with the usual comparisons. The results of the present work agree very well with both the DCS and the BR calculations, and we note that the theoretical Xαdipole moment, though it has the correct sign, has twice the experimental magnitude. This is not a serious discrepancy, however, since the dipole moment function of CO passes through zero very close to r_e (Chakerian Jr. 1976) and therefore has a relatively small magnitude there. The calculated first derivative, on the other hand, agrees very well with the experimental value.

Finally, let us consider the quadrupole moments of the homonuclear molecules N_2 and O_2, the only cases (of those

studied here) for which reliable experimental data are available. In Table 6.7 we compare the quadrupole moments of this work with experiment and with the results of Hartree-Fock calculations (quadrupole moments were not reported by GHJ, BR or DCS). We observe that both the present results and the Hartree-Fock results show fairly good agreement with experiment.

Table 6.3

Dissociation Energies D_e (eV)

	Expt	PW	DCS	BR	GHJ	HF
B_2	3.0	3.8	3.9			0.9
C_2	6.3	6.2	6.0			0.8
N_2	9.9	9.6	9.2	8.4	5.6	5.2
CO	11.2	12.1	12.0	11.5	8.3	7.8
O_2	5.2	7.1	7.0	6.6		1.3
F_2	1.7	3.3	3.2	2.9	0.3	-1.4

Expt: Experiment, Huber (1972)
PW : Present Work
DCS : Dunlap, Connolly and Sabin (1979)
BR : Baerends and Ros (1978)
GHJ : Gunnarsson, Harris and Jones (1977)
HF : Hartree-Fock;
Cade and Wahl (1974) (B_2,C_2,N_2,O_2,F_2)
Cade and Huo (1975) CO
Clementi and Roetti (1974) (atoms).

Table 6.4

Bond Lengths r_e (bohr)

	Expt	PW	DCS	BR	GHJ	HF
B_2	3.00	3.04	3.04			
C_2	2.35	2.36	2.35			2.37
N_2	2.07	2.06	2.08	2.13	2.16	2.01
CO	2.13	2.12	2.13	2.15	2.22	2.08
O_2	2.28	2.26	2.28	2.36		2.18
F_2	2.68	2.61	2.61	2.67	2.91	2.50

Expt: Experiment, Huber (1972)
PW : Present Work
DCS : Dunlap, Connolly and Sabin (1979)
BR : Baerends and Ros (1978)
GHJ : Gunnarsson, Harris and Jones (1977)
HF : Hartree-Fock, as given by DCS.

Table 6.5

Vibrational Frequencies ω_e (cm^{-1})

	Expt	PW	DCS	BR	GHJ	HF
B_2	1051	1020	1050			
C_2	1855	1870	1920			1970
N_2	2358	2380	2370	2360	2060	2730
CO	2170	2170	2160	2300	2000	2430
O_2	1580	1620	1610	1570		2000
F_2	892	1060	1090	1070	840	1260

Expt: Experiment, Huber (1972)
PW : Present Work
DCS : Dunlap, Connolly and Sabin (1979)
BR : Baerends and Ros (1978).
GHJ : Gunnarsson, Harris and Jones (1977)
HF : Hartree-Fock, as given by DCS.

Table 6.6

Dipole Moment Function of CO

	Expt	PW	DCS	BR	GHJ	HF
μ_0	-0.12	-0.25	-0.24	-0.25	-0.03	+0.27
μ_1	1.66	1.73	1.65	1.66	1.72	2.71

μ_0 = Dipole Moment (debye) (C^+O^-)

μ_1 = Dipole Moment Derivative (debye/bohr)

Expt : Experiment, Chakerian Jr. (1976)
PW : Present Work
DCS : Dunlap, Connolly and Sabin (1979)
BR : Baerends and Ros (1978)
GHJ : Gunnarsson, Harris and Jones (1977)
HF : Hartree-Fock, as given by DCS.

Table 6.7

Quadrupole Moments Q (10^{-26} esu cm^2)

$$Q = \frac{1}{2} \int \rho(3z^2-r^2)\ dv$$

	Expt	PW	HF
N_2	-1.4	-1.54	-1.36
O_2	-0.4	-0.51	-0.59

Expt: Experiment,
Buckingham, Disch and Dunmur (1968)

PW : Present Work

HF : Hartree-Fock,
Cade et al, reported by Stogryn
and Stogryn (1966).

6.4 Conclusions

The numerical method developed in this work has been shown in Section 6.2 to perform extremely well for the first row molecules considered here, and we have established an error limit of 0.1 eV on the energies reported in Table 6.3. We feel, therefore, that the present results accurately represent the Hartree-Fock-Slater theory.

Based on the comparisons of Section 6.3, we conclude that the Hartree-Fock-Slater theory, though very simple, describes molecular systems remarkably well. It certainly performs as well as (or even better than) the Hartree-Fock approximation, although the latter offers the advantage of being a proper "ab initio" theory.

The exchange parameter α has been somewhat arbitrarily chosen in these calculations, but reasonable adjustments of its value are not expected to affect the present results substantially. In the case of the N_2 molecule, for example, Dunlap, Connolly and Sabin (1979) report that a change in the value of α from 0.7 to the Schwarz (1972) value of 0.752 has the following consequences:

$$\Delta D_e = 0.17 \text{ eV}$$

$$\Delta r_e = -0.03 \text{ bohr}$$

$$\Delta \omega_e = 70 \text{ cm}^{-1} .$$

Clearly, the Hartree-Fock-Slater theory deserves further study and refinement, and the numerical method developed in this work may play an important role in these future studies.

Since the present numerical method is completely free of any model dependent error, the results of this work can also be used to assess the existing muffin-tin, cellular or LCAO computational schemes. In this regard, we note that the GTO-LCAO-Xα method of Dunlap, Connolly and Sabin (1979) produces results in excellent agreement with the present work, which confirms that the "Xα limit" has indeed been reached, at least for first row systems.

Furthermore, the DVM-LCAO results of Baerends and Ros (1978) are evidently more accurate than the LCMTO results of Gunnarsson, Harris and Jones (1977), but they nevertheless show significant discrepancies in comparison with the present work. Direct comparisons with other non-muffin-tin calculations (see Section 1.1) will not be made here since they generally employ values for the exchange parameter α different from the value $\alpha = 0.7$ used in these calculations.

Unfortunately, the present numerical technique cannot be directly extended to polyatomic systems, although many of the basic ideas of this work would certainly be useful in such an endeavour. The difficulty lies in the construction of completely orthogonal three-dimensional coordinate systems for multi-centre

geometries. It is this orthogonality which gives the present formalism its great simplicity, and gives the resulting matrix eigenvalue problem for the molecular orbitals the sparse block structure of Figure 4.1. Construction of such coordinate systems, however, is rather difficult for non-diatomic (or at least non-axially symmetric) molecules.

In the meantime, however, accurate numerical tests of Hartree-Fock-Slater and other density functional theories are now possible on the simplest of molecular systems: the diatomic molecule.

APPENDIX A

ASYMPTOTIC BEHAVIOUR OF THE TRANSFORMATION $\varepsilon_1(x_1)$

In Section 3.2 the coordinate transformation $\varepsilon_1(x_1)$ is defined in order to map the semi-infinite domain of ε_1 into the finite domain of the variable x_1. It was stated that a suitable transformation for this purpose is given by

$$\varepsilon_1 = c_1 \tanh^{-1}(x_1)$$

$$= \frac{c_1}{2} \ln\left(\frac{1+x_1}{1-x_1}\right) \qquad \text{(A.1a)}$$

where

$$0 \leq x_1 \leq 1 \, . \qquad \text{(A.1b)}$$

When making transformations of this kind, there is danger that certain volume integrals may become divergent, and therefore we shall investigate the asymptotic behaviour of expression (A.1) to ensure that all relevant integrals remain non-singular under this particular transformation. For convenience, we begin by defining the new variable

$$z = 1 - x_1 \qquad \text{(A.2)}$$

such that $z = 0$ corresponds to the asymptotic region. Then, from expression (A.1) we obtain the following asymptotic behaviour for ε_1 as z approaches zero:

$$\varepsilon_1 \sim -\frac{c_1}{2} \ln z \ . \qquad (A.3)$$

This behaviour is expressed in terms of the distance r using equation (3.3):

$$r \sim e^{\varepsilon_1} \sim z^{-c_1/2} \ . \qquad (A.4)$$

In the asymptotic limit, therefore, r and z are simply inverse powers of each other.

Now let us consider the large r behaviour of the volume integral of some arbitrary function F. The integrand asymptotically approaches

$$Fdv \sim F(r) r^2 dr \qquad (A.5)$$

where angular factors have been neglected. Recalling the integrals which are treated in this work, we find that two classes of behaviour for F(r) exist. First of all, we have a large number of integrals which contain orbitals or densities in their integrands, and in these cases we have

$$Fdv \sim e^{-\alpha r} dr \qquad (A.6)$$

which, using (A.4), can be written as

$$Fdv \sim r^{(1+2/c_1)} e^{-\alpha r} dz \ . \qquad (A.7)$$

This expression is, of course, well-behaved at $r \to \infty$ for all positive values of c_1 and α.

In connection with the Poisson equation, however, we

encounter the integral (5.9) with the integrand $F = (\nabla V_{el})^2$. Recalling the asymptotic behaviour (5.34) of the coulomb potential, we obtain in this case

$$Fdv \sim r^{-4}dr \ . \tag{A.8}$$

Again using (A.4), this expression is rewritten as

$$Fdv \sim z^{(3c_1/2-1)}dz \ . \tag{A.9}$$

This time, however, we notice that (A.9) <u>diverges</u> at $z = 0$ unless

$$c_1 > 2/3 \tag{A.10}$$

which, using (3.8b) and (3.9), implies that

$$\frac{r_m}{a} > \cosh\left(\frac{\ell n 3}{3}\right) - 1 > 0.068 \ . \tag{A.11}$$

Fortunately, this condition is easily satisfied for typical molecular internuclear distances, and we need concern ourselves with (A.11) only when the internuclear separation becomes very large.

The transformation (A.1), therefore, may be safely employed in the present work.

APPENDIX B

CALCULATION OF THE DISCRETE DIFFERENTIATION MATRICES AND INTEGRATION WEIGHTS

In Section 3.4 we describe discrete differentiation matrices $d^{(1)}$ and $d^{(2)}$ and integration weights $w^{(1)}$ and $w^{(2)}$ for the x_1 and x_2 meshes, and in this appendix the calculation of these objects will be outlined. For convenience in the following work, the mesh superscript is neglected since formulae for either the x_1 or the x_2 meshes have identical form.

Given an arbitrary function F on a discrete one-dimensional mesh, the differentiation matrix d and the integration weights w are defined as follows:

$$\left.\frac{dF}{dx}\right|_i \simeq \sum_j d_{ij} F_j \qquad \text{(B.1a)}$$

$$\int F(x)dx \simeq \sum_i w_i F_i \ . \qquad \text{(B.1b)}$$

These expressions may be written in much more compact form by defining the column vectors F, F' and w in the obvious manner. In terms of these vectors, equations (B.1) may be written as

$$F' = dF \qquad \text{(B.2a)}$$

and

$$\int F(x)dx = w^T F \qquad \text{(B.2b)}$$

where d is the differentiation matrix of (B.1a) and the superscript T denotes matrix transposition. We shall use this vector-matrix notation throughout the remainder of this section.

In the present work the matrix d and the vector w are calculated using spline analysis, and the particular method employed here is based on the B-spline theory outlined, for example, by Prenter (1975, ch. 4). The general theory of B-splines is discussed briefly in Appendix D, and for the moment, we need only know that nth order B-splines are basis functions for the space of all possible nth order spline functions on a uniform mesh.

Then, using third order (cubic) B-splines in Appendix E, we construct a set of basis functions ϕ_i and their corresponding derivative functions θ_i for each of the x_1 and the x_2 meshes, as well as matrices ϕ_{ij} and θ_{ij} such that, for example, ϕ_{ij} denotes the value of ϕ_i at the mesh point j. These matrices are tridiagonal, and in addition, the matrix ϕ is symmetric.

We also define the column vector s, such that

$$s_i = \int \phi_i(x)dx \ . \qquad (B.3)$$

Using the preceding definitions, we write the following expressions for the function F, its derivative, and its integral in terms of the basis set expansion coefficients "a":

$$F = \phi a \qquad (B.4)$$

and

$$F' = \theta^T a \tag{B.5a}$$

$$\int F(x)dx = s^T a \ . \tag{B.5b}$$

Although these equations give the derivative and integral of F in terms of the expansion coefficients "a", we desire expressions for these quantities in terms of the vector F itself.

This is, in fact, easily accomplished by inverting equation (B.4):

$$a = \phi^{-1} F \tag{B.6}$$

and then substituting this expression into (B.5) to obtain

$$F' = \theta^T \phi^{-1} F \tag{B.7a}$$

$$\int F(x)dx = s^T \phi^{-1} F \ . \tag{B.7b}$$

These equations have the desired form (B.2), and by inspection we immediately write

$$d = \theta^T \phi^{-1} \tag{B.8a}$$

$$w^T = s^T \phi^{-1} \tag{B.8b}$$

which give the differentiation matrix and the integration weights in simple terms of the cubic spline basis matrices of Appendix E.

As mentioned in Section 3.4, this particular derivation of the matrices $d^{(1)}$ and $d^{(2)}$ and the weights $w^{(1)}$ and $w^{(2)}$ is not an essential ingredient of the present method. Any other desired numerical technique can be used to compute them (i.e. finite differences, higher order splines, trigonometric interpolation, etc.). The formalism of Chapter 4 and Section 5.1 is quite independent of the precise choice of this numerical input, provided that the definitions (B.1) are satisfied.

We have chosen to work with cubic B-splines in these calculations because of their great efficiency in solving the Poisson equation by the method of Section 5.2.

APPENDIX C

THE LANCZOS ALGORITHM

In Chapter 4, the determination of the molecular orbitals was reduced to a symmetric matrix eigenvalue problem of the form

$$AX = X\lambda \tag{C.1}$$

where the columns of matrix X are the eigenvectors of A, and λ is a diagonal matrix containing the corresponding eigenvalues. As discussed in Section 4.4, the coefficient matrix A is very sparse, and furthermore, excellent approximations for the eigenvectors exist at the outset of each self-consistent iteration. Therefore, iterative numerical methods for the solution of eigenvalue problems are ideal for our purposes, and in this work the so-called Lanczos method has been used (Lanczos 1950). A nice discussion of the method is given by Fox (1964, pgs. 252,270).

Essentially, the Lanczos algorithm iteratively generates a similarity transformation from matrix A to a tridiagonal matrix C, where

$$AY = YC \tag{C.2}$$

and C is assumed to be symmetric, having the form

$$C = \begin{vmatrix} \alpha_1 & \beta_2 & & & \\ \beta_2 & \alpha_2 & \beta_3 & & \\ & \beta_3 & \alpha_3 & \beta_4 & \\ & & \beta_4 & \alpha_4 & \\ & & & \text{etc.} & \end{vmatrix} . \qquad (C.3)$$

Since A and C are both symmetric, the columns of the transformation matrix Y, denoted y_r, are orthonormal.

Using (C.3), the rth column of the matrix equation (C.2) can be written as

$$Ay_r = \beta_r y_{r-1} + \alpha_r y_r + \beta_{r+1} y_{r+1} \qquad (C.4)$$

or, rearranging slightly,

$$\beta_{r+1} y_{r+1} = Ay_r - \alpha_r y_r - \beta_r y_{r-1} . \qquad (C.5)$$

This equation gives the column y_{r+1} in terms of the two previous columns y_r and y_{r-1}. Since y_{r+1} is orthogonal to y_r, we obtain

$$\alpha_r = y_r^T A y_r \qquad (C.6)$$

which follows from (C.5) if we multiply by y_r^T and use the fact that y_r is orthogonal to y_{r-1}. The value of β_{r+1} is then determined by properly normalizing column y_{r+1}. Beginning with $y_0 = 0$, therefore, and a starting vector y_1, equation (C.5) iteratively generates the columns of the transformation matrix.

As discussed by Paige (1972), this procedure works if certain precautions are taken, but in general the columns of Y

eventually lose their orthogonality due to roundoff error in the subtraction (C.5). Therefore, in the present work, the columns y_r have been explicitly reorthogonalized in a manner described by Whitehead et al (1977, sec. 2):

First of all, we calculate

$$y'_{r+1} = Ay_r - \alpha_r y_r - \beta_r y_{r-1} \qquad (C.7)$$

where α_r is given by (C.6) and β_r comes from the previous iteration. Then, we explicitly orthogonalize y'_{r+1} with respect to all previous columns using

$$\beta_{r+1} y_{r+1} = y'_{r+1} - \sum_{s=1}^{r} \varepsilon_s y_s \qquad (C.8)$$

where

$$\varepsilon_s = y_s^T y'_{r+1} . \qquad (C.9)$$

Then, finally, β_{r+1} is chosen such that the new column y_{r+1} is normalized, and the procedure is repeated by returning to (C.7).

When the tridiagonal matrix C has been produced, the much simpler problem

$$CZ = Z\lambda \qquad (C.10)$$

may be solved using well known and efficient numerical algorithms for tridiagonal eigenvalue problems (such as routines RATQR and TINVIT from the EISPACK library of Smith et al 1974).

Then, multiplying equation (C.10) by the matrix Y and using (C.2) to obtain

$$A(YZ) = (YZ)\lambda \tag{C.11}$$

we observe that the eigenvectors of the original problem (C.1) are related to the eigenvectors of the tridiagonal problem (C.10) by

$$X = YZ \ . \tag{C.12}$$

Therefore, the Lanczos algorithm conveniently reduces the initial eigenvalue problem to a much more simple tridiagonal form.

For an arbitrary choice of starting vector y_1, the Lanczos procedure with reorthogonalization is actually less efficient than other well known tridiagonalization methods such as Householder or Givens. If the vector y_1 is properly chosen, however, then the Lanczos algorithm may, in fact, be truncated after surprisingly few iterations, and herein lies the real power of the method.

In order to understand this, suppose that y_1 is a linear combination of the m lowest eigenstates of matrix A, where m is small compared to the order of the matrix. The Lanczos algorithm in this case would terminate after m iterations, having generated the m-dimensional subspace of the m lowest eigenvectors. If, however, y_1 is a linear combination of approximate eigenvectors, then the Lanczos procedure never terminates but it nevertheless produces rapidly convergent

results for the lowest m eigenstates.

In a self-consistent calculation then, if y_1 is the sum of the orbitals from the previous self-consistent cycle, this convergence is very fast, especially as self-consistency is achieved. This remarkable property of the Lanczos method is nicely illustrated by Hoodbhoy and Negele (1977) for numerical Hartree-Fock calculations on axially symmetric nuclei.

The Lanczos algorithm is therefore tremendously efficient for the calculation of molecular orbitals in the present work, and very large numbers of mesh points (up to a thousand or so) can be handled.

APPENDIX D

B-SPLINES

In this appendix we shall very briefly outline the general theory of nth order spline functions. A much more thorough discussion is given in the book by Prenter (1975).

Let us begin by defining exactly what is meant by the term "spline function". Assume, first of all, that we are given a discrete one-dimensional mesh not necessarily uniform, on some finite domain of the variable x. An nth order spline function is a function, well-behaved in each mesh interval, which, at the mesh points, has continuous value and continuous derivatives up to and including order (n-1) but not necessarily beyond. In other words, a spline function is a piecewise continuous function with "smoothness" constraints on the lower order derivatives applied at the mesh points. In the case of an nth order <u>polynomial</u> spline, the function is represented in each interval by a polynomial of order n.

From the above definition, it is clear that a linear combination of spline functions is also a spline function, and therefore it is possible to define <u>basis</u> splines for the space of nth order spline functions on a given mesh. One such class of basis splines are the so-called B-splines, which are characterized by the fact that they are maximally "localized" on the mesh.

Let us consider the general properties of an nth order polynomial B-spline on a uniform mesh with interval h. Assume, first of all, that the B-spline is non-zero over ℓ intervals, and vanishes everywhere else. Since it is represented by an nth order polynomial in each interval, we have a total of $\ell(n+1)$ undetermined coefficients altogether. The continuity conditions at each mesh point, however, impose a total of $n(\ell+1)$ constraints. Therefore, the constraints being homogeneous, it is clear that the number of undetermined coefficients should exceed the number of constraints by exactly <u>one</u>, if a unique solution (within a normalization constant) is desired. Consequently, we see that an nth order polynomial B-spline is uniquely defined over <u>$\ell = n+1$</u> intervals and vanishes elsewhere.

The preceding argument shows that a polynomial B-spline of order n spans (n+1) intervals, from mesh point x_0, say, to the mesh point x_{n+1}. It can be shown that the B-spline on this interval is explicitly given by the following expression:

$$B(x) = \frac{1}{h^n} \sum_{k=0}^{n} (-1)^k \binom{n+1}{k} (x-x_k)_+^n \qquad (D.1)$$

where $\binom{n+1}{k}$ is the usual binomial coefficient, and the function $(x-x_k)_+^n$ is defined by

$$(x-x_k)_+^n = \begin{cases} (x-x_k)^n & , \quad x \geq x_k \\ 0 & , \quad x < x_k \end{cases} \qquad (D.2)$$

and is itself an nth order spline function. It is not difficult to verify that expression (D.1) does, indeed, have all of the requisite properties of an nth order B-spline.

We are particularly interested in the values of $B(x)$, its derivatives, and its integral at the mesh points x_p. Using (D.1) we compile the following results:

$$B(x_p) = \sum_{k=0}^{(p-1)} (-1)^k \binom{n+1}{k} (p-k)^n \qquad (D.3)$$

$$\left(\frac{d}{dx}\right)^m B(x_p) = \frac{n!}{(n-m)!h^m} \sum_{k=0}^{(p-1)} (-1)^k \binom{n+1}{k} (p-k)^{n-m} \qquad (D.4)$$

$$\int_{x_0}^{x_p} B(x)dx = \frac{h}{(n+1)} \sum_{k=0}^{(p-1)} (-1)^k \binom{n+1}{k} (p-k)^{n+1} . \qquad (D.5)$$

Notice that the normalization has been chosen in such a way that $B(x_1) = B(x_n) = 1$.

A complete basis set for the expansion of an arbitrary nth order spline function on a uniform mesh is constructed by associating one such B-spline with each mesh point, and we shall construct such bases using cubic B-splines in Appendix E.

APPENDIX E

THE CUBIC B-SPLINE BASIS

General formulae were given in the previous appendix for the nth order B-spline on a uniform mesh, and we shall now specialize these formulae to the case of cubic splines which are used in the present work.

The cubic B-splines extend over four intervals, and we denote the B-spline centred on the ith mesh point as $B_i(x)$. Using expressions (D.3), (D.4) and (D.5) of the previous appendix, we complete the following table:

Table E.1

$p =$	$i-2$	$i-1$	i	$i+1$	$i+2$
$B_i(x_p) =$	0	1	4	1	0
$\frac{d}{dx} B_i(x_p) =$	0	$3/h$	0	$-3/h$	0
$\int_{x_{i-2}}^{x_p} B_i(x)dx =$	0	$h/4$	$3h$	$23h/4$	$6h$

The cubic B-spline $B_i(x)$ is illustrated on the following page in Figure E.1.

Figure E.1

Sketch of the Cubic B-Spline $B_i(x)$.

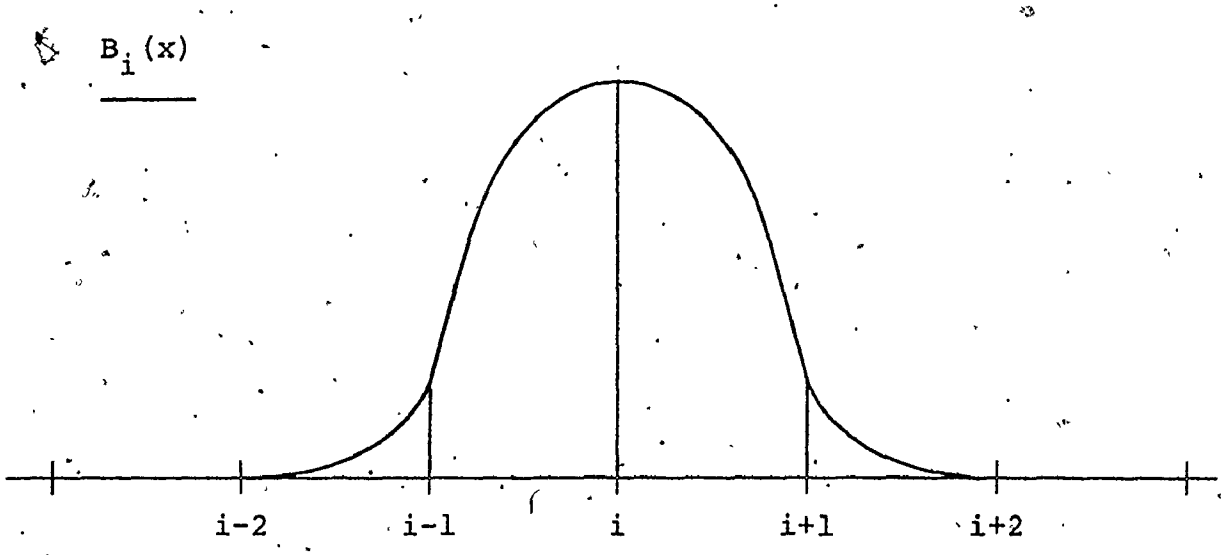

In order to incorporate the boundary conditions of Section 3.3, we form linear combinations of these cubic B-splines to construct the basis functions ϕ_i of Appendix B and Section 5.2. We give these linear combinations below, and refer the reader to Sections 3.3 and 3.4 for a review of the meshes and boundary conditions:

(Note that, throughout this work, the function μ defined by (4.7), (4.29) and (5.3) has π symmetry.)

x_1 Mesh:

$$\phi_1 = B_1 - B_{-1}$$
$$\phi_i = B_i \qquad \text{for } i = 2 \text{ to } (N-1) \qquad (N = N_1)$$
$$\phi_N = B_N + B_{N+2} - \frac{1}{2} B_{N+1}$$

x_2 Mesh (Heteronuclear Molecules):

$$\phi_1 = B_1 - B_{-1}$$
$$\phi_i = B_i \qquad \text{for } i = 2 \text{ to } (N-1) \qquad (N = N_2)$$
$$\phi_N = B_N - B_{N+2}$$

x_2 Mesh (Homonuclear Molecules):

$$\phi_1 = B_1 - B_{-1}$$
$$\phi_i = B_i \qquad \text{for } i = 2 \text{ to } (N-2) \qquad (N = N_2)$$
$$\phi_{N-1} = B_{N-1} \pm B_{N+2}$$
$$\phi_N = B_N \pm B_{N+1}$$

(where the $\pm$ sign depends on the reflection symmetry of the state in question.)

These expressions for the basis functions ϕ_i, along with Table E.1, are used to calculate the matrices ϕ_{ij} and θ_{ij} and the vector s_i of Appendix B and Section 5.2. Their calculation is straightforward and is therefore not reproduced

here. We note, however, that the matrices ϕ and θ are both tridiagonal, and this simplifies the solution of the Poisson equation in Section 5.2 tremendously.

REFERENCES

Anderson O.K. and Woolley R.G. (1973) Mol. Phys. 26, 905.

Arfken G.B. (1970) "Mathematical Methods for Physicists, 2nd Ed.", Academic Press, New York.

Baerends E.J., Ellis D.E. and Ros P. (1973) Chem. Phys. 2, 41.

Baerends E.J. and Ros P. (1973) Chem. Phys. 2, 52.

Baerends E.J. and Ros P. (1975) Chem. Phys. 8, 412.

Baerends E.J. and Ros P. (1978) Int. J. Quantum Chem. S12, 169.

Brescansin L.M., Leite J.R. and Ferreira L.G. (1979) J. Chem. Phys. 71, 4923.

Buckingham A.D., Disch R.L. and Dunmur D.A. (1968) J. Am. Chem. Soc. 90, 3104.

Cade P.E. and Huo W.M. (1975) At. Data Nucl. Data 15, 1.

Cade P.E. and Wahl A.C. (1974) At. Data Nucl. Data 13, 339.

Chakerian Jr. C. (1976) J. Chem. Phys. 65, 4228.

Christiansen P.A. and McCullough Jr. E.A. (1977) J. Chem. Phys. 67, 1877.

Clementi E. and Roetti C. (1974) At. Data Nucl. Data 14, 177.

Costas M. and Garritz A. (1979) Int. J. Quantum Chem. S13, 141.

Danese J.B. (1974) J. Chem. Phys. 61, 3071.

Danese J.B. (1977) Chem. Phys. Lett. 45, 150.

Danese J.B. and Connolly J.W.D. (1974) J. Chem. Phys. 61, 3063.

Dunlap B.I., Connolly J.W.D. and Sabin J.R. (1979) J. Chem. Phys. 71, 3396 and 4993.

Ellis D.E. and Painter G.S. (1970) Phys. Rev. B2, 2887.

Fox L. (1964) "An Introduction to Numerical Linear Algebra", Clarendon Press, Oxford.

Gaspar R. (1954) Acta Phys. Acad. Sci. Hung. 3, 263.

Gasquez J.L. and Keller J. (1977) Phys. Rev. A16, 1358.

Gopinathan M.S., Whitehead M.A. and Bogdanovic R. (1976) Phys. Rev. A14, 1.

Gunnarsson O., Harris J. and Jones R.O. (1977) J. Chem. Phys. 67, 3970.

Gunnarsson O. and Johansson P. (1976) Int. J. Quantum Chem. 10, 307.

Heijser W., Van Kessel A.Th. and Baerends E.J. (1976) Chem. Phys. 16, 371.

Herman F. and Skillman S. (1963) "Atomic Structure Calculations", Prentice-Hall, Englewood Cliffs.

Herman F., Williams A.R. and Johnson K.H. (1974) J. Chem. Phys. 61, 3508.

Hoodbhoy P. and Negele J.W. (1977) Nucl. Phys. A288, 23.

Huber K.P. (1972) Sec. 7g of "American Institute of Physics Handbook", Edited by Gray D.E., McGraw-Hill, New York.

Johnson K.H. (1966) J. Chem. Phys. 45, 3085.

Johnson K.H. (1973) Adv. Quantum Chem. 7, 143.

Johnson K.H. (1975) Ann. Rev. Phys. Chem. 26, 39.

Keller J. (1975) Int. J. Quantum Chem. 9, 583.

Kohn W. and Rostoker N. (1954) Phys. Rev. 94, 1111.

Kohn W. and Sham L.J. (1965) Phys. Rev. 140, A1133.

Korringa J. (1947) Physica 13, 392.

Lanczos C. (1950) J. Res. Nat. Bur. Stand. 45, 255.

McCullough Jr. E.A. (1974) Chem. Phys. Lett. 24, 55.

McCullough Jr. E.A. (1975) J. Chem. Phys. 62, 3991.

Paige C.C. (1972) J. Inst. Math. Applic. 10, 373.

Prenter P.M. (1975) "Splines and Variational Methods", Wiley, New York, Toronto.

Roothaan C.C.J. (1951) Rev. Mod. Phys. 23, 69.

Rosch N., Klemperer W.G. and Johnson K.H. (1973) Chem. Phys. Lett. 23, 149.

Rosenkrantz M.E. and Konowalow D.D. (1979) Int. J. Quantum Chem. 16, 1301.

Salahub D.R., Messmer R.P. and Johnson K.H. (1976) Mol. Phys. 31, 529.

Sambe H. and Felton R.H. (1975) J. Chem. Phys. 62, 1122.

Schwarz H.R. (1973) "Numerical Analysis of Symmetric Matrices", Prentice-Hall, Englewood Cliffs.

Schwarz K. (1972) Phys. Rev. B5, 2466.

Slater J.C. (1937) Phys. Rev. 51, 846.

Slater J.C. (1951) Phys. Rev. 81, 385.

Slater J.C. (1965) J. Chem. Phys. 43, S228.

Slater J.C. (1972) Adv. Quantum Chem. 6, 1.

Slater J.C. (1974) "Quantum Theory of Molecules and Solids", Vol. 4: "The Self-Consistent Field for Molecules and Solids", McGraw-Hill, New York.

Smith B.T., Boyle J.M., Garbow B.S., Ikebe Y., Klema V.C. and Moler C.B. (1974) "Matrix Eigensystem Routines-EISPACK Guide", Springer-Verlag, Berlin,New York.

Stogryn D.E. and Stogryn A.P. (1966) Mol. Phys. 11, 371.

Tinkham M. (1964) "Group Theory and Quantum Mechanics", McGraw-Hill, New York.

Whitehead R.R., Watt A., Cole B.J. and Morrison I. (1977) Adv. Nucl. Phys. 9, 123.

Williams A.R. (1974) Int. J. Quantum Chem. S8, 89.

Ziegler T., Rauk A. and Baerends E.J. (1977) Theoret. Chim. Acta 43, 261.